J Neurophysiol 122: 872–887, 2019.
First published July 10, 2019; doi:10.1152/jn.00167.2019.

RESEARCH ARTICLE | *Control of Movement*

Differential activation of lumbar and sacral motor pools during walking at different speeds and slopes

A. H. Dewolf,[1] Y. P. Ivanenko,[2] K. E. Zelik,[2,3,4,5] F. Lacquaniti,[2,6] and P. A. Willems[1]

[1]*Laboratory of Biomechanics and Physiology of Locomotion, Institute of NeuroScience, Université catholique de Louvain, Louvain-la-Neuve, Belgium;* [2]*Laboratory of Neuromotor Physiology, IRCCS Santa Lucia Foundation, Rome, Italy;* [3]*Department of Mechanical Engineering, Vanderbilt University, Nashville, Tennessee;* [4]*Department of Biomedical Engineering, Vanderbilt University, Nashville, Tennessee;* [5]*Department of Physical Medicine and Rehabilitation, Vanderbilt University, Nashville, Tennessee; and* [6]*Department of Systems Medicine and Center of Space Biomedicine, University of Rome Tor Vergata, Rome, Italy*

Submitted 13 March 2019; accepted in final form 28 June 2019

Dewolf AH, Ivanenko YP, Zelik KE, Lacquaniti F, Willems PA. Differential activation of lumbar and sacral motor pools during walking at different speeds and slopes. *J Neurophysiol* 122: 872–887, 2019. First published July 10, 2019; doi:10.1152/jn.00167.2019.—Organization of spinal motor output has become of interest for investigating differential activation of lumbar and sacral motor pools during locomotor tasks. Motor pools are associated with functional grouping of motoneurons of the lower limb muscles. Here we examined how the spatiotemporal organization of lumbar and sacral motor pool activity during walking is orchestrated with slope of terrain and speed of progression. Ten subjects walked on an instrumented treadmill at different slopes and imposed speeds. Kinetics, kinematics, and electromyography of 16 lower limb muscles were recorded. The spinal locomotor output was assessed by decomposing the coordinated muscle activation profiles into a small set of common factors and by mapping them onto the rostrocaudal location of the motoneuron pools. Our results show that lumbar and sacral motor pool activity depend on slope and speed. Compared with level walking, sacral motor pools decrease their activity at negative slopes and increase at positive slopes, whereas lumbar motor pools increase their engagement when both positive and negative slope increase. These findings are consistent with a differential involvement of the lumbar and the sacral motor pools in relation to changes in positive and negative center of body mass mechanical power production due to slope and speed.

NEW & NOTEWORTHY In this study, the spatiotemporal maps of motoneuron activity in the spinal cord were assessed during walking at different slopes and speeds. We found differential involvement of lumbar and sacral motor pools in relation to changes in positive and negative center of body mass power production due to slope and speed. The results are consistent with recent findings about the specialization of neuronal networks located at different segments of the spinal cord for performing specific locomotor tasks.

modular control; muscle activity; neuromechanics; spinal maps; walking on slopes

INTRODUCTION

The final output of the locomotor circuitry comprising supraspinal, sensory, and central pattern generator (CPG) signals is represented by the spatiotemporal modulation of α-motoneuron (MN) activity (Brown 1914; Grillner 1981; Kiehn 2016). In the course of evolution, motor circuits in the spinal cord were assembled to meet specific body movement requirements and specific spatial arrangement and biomechanical function of limb muscles (Jessell et al. 2011). A sequential trunk muscle activation for the undulatory body movements (de Sèze et al. 2008) was replaced by more complex and discrete bursts of limb MN activity related to specific kinematic and kinetic events (Lacquaniti et al. 2012). Each human lower limb contains >50 muscles, and corresponding MNs are grouped in motor columns (Sharrard 1964) whose spatiotemporal organization is precisely orchestrated during development (Dewitz et al. 2018). Furthermore, motor pool topography contributes to sensory-motor connectivity in the spinal cord (Jessell et al. 2011).

In recent years, there has been growing interest in understanding the functional organization of the spinal locomotor output in the context of neuromodulation of the spinal circuitry (Taccola et al. 2018; Wenger et al. 2016), differential impairment of lumbar and sacral motor pools in gait pathologies (Coscia et al. 2015; Grasso et al. 2004; Martino et al. 2018), and adaptation to different biomechanical requirements (Allen and Franz 2018; Chvatal et al. 2011; Ivanenko et al. 2008; MacLellan et al. 2012; Martino et al. 2015; Santuz et al. 2018). Furthermore, selective stimulation of spinal motor pools represents a promising tool to restore the functioning of the spinal pattern generation circuitry in both animals (Capogrosso et al. 2016; Wenger et al. 2016) and humans (Angeli et al. 2018; Gerasimenko et al. 2015; Solopova et al. 2017; Wagner et al. 2018). Overall, these findings highlight the importance of investigating the functional segmental organization and biomechanical functions of lumbar and sacral motor pools.

Only a few studies have attempted to evaluate the relationship between the spatiotemporal organization of the spinal motor output and biomechanics in human locomotion (Cappellini et al. 2010; La Scaleia et al. 2014; MacLellan et al. 2012;

Address for reprint requests and other correspondence: P. A. Willems, UCL-FSM, Place P. de Coubertin, 1, B-1348 Louvain-la-Neuve, Belgium (e-mail: patrick.willems@uclouvain.be).

Martinez-Valdes et al. 2018; Yokoyama et al. 2017). During walking, the spatiotemporal organization of the spinal motor pools fluctuates roughly in phase with the motion of the center of body mass (COM) (Cappellini et al. 2010), with bursts of activity around touchdown and foot liftoff (La Scaleia et al. 2014). In particular, biomechanical mechanisms of locomotion, such as inverted pendulum walking dynamics, are related to specific spatiotemporal organization of motor pool activity in the spinal cord (Cappellini et al. 2010). To further investigate the relationships between bursts of MN activity and biomechanical functions, here we examine how the spatiotemporal dynamics of motor pool activity is related to human walking on different slopes and at different speeds.

Recently, we reported modifications in walking biomechanics with slopes (Dewolf et al. 2017, 2018). The changes in the mechanical demands induced modifications in the neuromuscular control during slope compared with level walking (Janshen et al. 2017; Rozumalski et al. 2017; Saito et al. 2018). In particular, Lay et al. (2007) observed nonuniform changes in the muscle activity patterns across negative and positive slopes compared with level walking, suggesting that new control strategies are needed for walking on slopes. Furthermore, we reported a speed-dependent modification in the walking pattern on slopes (Dewolf et al. 2018), reflecting that there is no simple scaling of spinal motor output activity with speed and slope but the involvement of somewhat different neural circuits (Yokoyama et al. 2017).

In light of the above-mentioned considerations and a differential biomechanical function of lower limb muscles (Pickle et al. 2016), we expect that modifications in the spatiotemporal organization of motor pool activity in the lumbar and sacral spinal cord would be related to biomechanical changes due to slope and speed. A better understanding of the outputs of MN pools during different locomotor conditions may provide further insights into interspecies comparison (Carlson-Kuhta et al. 1998; Smith et al. 1998; Yakovenko et al. 2002) and into modularity of neural control in humans with changes in environmental demands (La Scaleia et al. 2014; Santuz et al. 2018). Knowledge about how the nervous system adapts to such demands in normal subjects can provide a basis for understanding deficits in patient populations and may thus have important clinical implications (Cappellini et al. 2016; Grasso et al. 2004; Wagner et al. 2018).

Specifically, we addressed the question of whether the pools of α-MNs are recruited in the same chronological order and relative intensity or are differentially activated as a function of speed and slope. The former case would be implied by the hypothesis that there exists a leading oscillator in the lumbar spinal cord that propagates motor bursts to more caudal segments by means of traveling waves of activity (Cazalets et al. 1995; Cuellar et al. 2009; Saltiel et al. 2016). The latter case, instead, would be implied by the hypothesis that there exist multiple generators of locomotor activity that can operate quasi-independently of each other (Grillner 1981; Hägglund et al. 2013).

The identification of CPGs in humans remains difficult, but one can obtain critical insights by describing the spatiotemporal activation of MN pools during locomotion (Ivanenko et al. 2006a). Spatiotemporal maps of activation are derived from recording electromyogram (EMG) activity profiles from several muscles of the lower limbs during walking and combining these profiles with known lumbosacral segmental organization of MN pools Kendall et al. 1993; Sharrard 1964).

We asked subjects to walk on an instrumented treadmill on inclined surfaces at different imposed velocities. Then, we assessed the spatiotemporal modulation of the MN output by mapping the activity patterns from a large number of simultaneously recorded muscles onto the anatomical rostrocaudal location of the MN pools in the spinal cord, which offers a compact representation of the total motor output (Ivanenko et al. 2006a, 2013b; O'Donovan et al. 2008; Monaco et al. 2010; Warp et al. 2012; Yakovenko et al. 2002). Then, we related the spatiotemporal modulation of the MNs to the kinetics of the COM, to explore relationships between changes in the mechanics of walking and changes in its motor control. In addition, we decomposed the coordinated muscle activation profiles into a small set of common factors. Such factor analysis identified the major neuromuscular activation patterns, allowing further assessment of differential changes in the motor output of the lumbosacral cord as a function of speed and slope.

METHODS

Participants and Experimental Protocol

We recorded surface EMGs at the same time and on the same subjects as in previous studies (Dewolf et al. 2017, 2018). Ten healthy subjects (6 men, 4 women; age: 22.2 ± 2.4 yr, mass: 69.2 ± 14.4 kg, height: 1.75 ± 0.10 m, means ± SD) walked on an instrumented treadmill at seven different inclinations (0°, ±3°, ±6°, and ±9°). Six of them walked on all slopes, two walked at 0° and ±6°, and two walked at 0° and ±9°. At each slope, subjects walked at seven different speeds ranging between 0.56 m/s (2 km/h) and 2.22 m/s (8 km/h); some subjects were not able to walk at 2.22 m/s at all slopes. Between 6 and 36 strides per trials were recorded, and a total of 8,864 strides were analyzed. Before participation, subjects gave written informed consent. The study followed the guidelines of the Declaration of Helsinki, and the procedures were approved by the Research Ethics Committee of the Université catholique de Louvain (Ref. No. 2015/06JUL/372).

Data Recordings

We recorded kinematic data at 100 frames/s with a high-speed video camera (Basler A501k; resolution 1,280 × 1,024 pixels, aperture time 3 ms) fixed on the ground 3 m to the side of the treadmill, perpendicular to the plane of progression. Reflective markers were placed on one side of the subject over the following landmarks: the chin-neck intersect, greater trochanter, lateral femoral epicondyle, lateral malleolus, heel, and fifth metatarsophalangeal joint. The instrumented treadmill measured the normal, parallel, and lateral components of the ground reaction force exerted by the tread belt on the feet. The force signals were digitized by a 16-bit analog-to-digital converter at 1,000 Hz. The vertical (v), fore-aft (y), and lateral components of force and velocity of the COM were then computed with the methods described in Dewolf et al. (2016).

We recorded EMG activity at 2,000 Hz by means of surface electrodes (using the Trigno Wireless EMG System; Delsys, Boston, MA; bandwidth of 20–450 Hz, overall gain of 1,000) from 16 muscles on the right side of each subject. These included one muscle from the lower back [erector spinae (ES) at L_2 level], two muscles from the buttocks [gluteus maximus (Gm) and gluteus medius (Gmed)], eight muscles from the thigh [sartorius (SART), tensor fasciae latae (TFL), adductor longus (ADD), vastus medialis (VM), vastus lateralis (VL), rectus femoris (RF), biceps femoris long head (BF), semitendinosus (ST)], and five muscles from the shank [tibialis

anterior (TA), medial gastrocnemius (MG), lateral gastrocnemius (LG), soleus (SOL), peroneus longus (PERL)]. After preparing the shaved skin with fine sandpaper, ether, and alcohol, we placed EMG electrodes (5-mm bar electrodes with a 10-mm interelectrode distance) based on suggestions from SENIAM (http://www.seniam.org), the European project on surface EMG. To this end, we located the muscle bellies by means of palpation and oriented the electrodes along the main direction of the fibers (Kendall et al. 2005; Winter 1991). We verified electrode position and signal quality by visually inspecting the EMG signals while subjects contracted each instrumented muscle and then also visually inspected EMG signals from the walking trials. Some EMG signals from these walking trials were not usable and were thus removed on a subject-specific basis. On average we analyzed 15.3 muscle EMGs from each subject in each condition.

Data Analysis

General gait parameters. The stride was defined as the period between two right foot contacts (FCs). FC and toe-off (TO) were defined based on the displacement of the center of pressure on the belt (Meurisse et al. 2016). The stride frequency (f) was calculated as the inverse of the time between two successive right FCs. We calculated the beginning of the step-to-step transition phase measuring the index of the minimum (t_v) of the vertical velocity of the COM V_v, as defined by Adamczyk and Kuo (2009). The duration of the double contact phase (t_{DC}) was determined as the time between FC and TO of the contralateral foot. Both t_v and t_{DC} were normalized relative to the stride duration.

Terminology for mechanical power. The mechanical power during walking can be estimated on one hand from the power done to move the COM relative to the surroundings plus the power done on/by the environment and on the other hand as the power developed to the move of the body segments relative to the COM. This division of the power into two parts was proposed for the first time by Fenn (1930) and was improved and popularized by Cavagna et al. (1963). In this "classical" division, the two parts are called external and internal power, respectively. However, this terminology can be misleading, since the terms "external and internal power" are used differently by many authors, as discussed in detail in van der Kruk et al. (2018). Furthermore, this terminology may be confusing because the internal and external powers are both performed "internally," i.e., within the body (mostly by muscle). To avoid any ambiguity, the terms used are clearly defined in the following section.

COM and peripheral power. The COM power, $\dot{W}_{com}$, referred as external power by Cavagna et al. (1963), can be computed by (Gosseye et al. 2010)

$$\dot{W}_{com} = \mathbf{FV} \quad (1)$$

where **F** and **V** are the force vector and the velocity vector of the COM, respectively. The pattern of fluctuation of the COM power during walking typically presents one major peak of negative power ($\dot{W}^-$) and two major peaks of positive power ($\dot{W}_1^+$ and $\dot{W}_2^+$) (Cavagna et al. 1976). Here, the maximum of each of these three peaks were measured across all conditions.

To compute the peripheral power $\dot{E}_{per}$, as named by van der Kruk et al. (2018) or Zelik and Kuo (2012) but also referred to as internal power by Cavagna and Kaneko (1977), the body was subdivided into seven rigid segments (trunk + arms + head, thighs, shanks, and feet) as in Davis et al. (1991), the position of the COM of the body was calculated from the position of the center of mass and the mass of each segment, as obtained from anthropometric tables (Dempster and Gaughran 1967). The translational and rotational velocity of the segments relative to the COM was then computed (Willems et al. 1995). $\dot{E}_{per}$ was then estimated as the time derivative of changes in the sum of the translational and rotational energy of each segment relative to the COM (E_{per}), computed as

$$E_{per} = \sum_{i=1}^{7} \frac{m_i v_{i,com}^2 + I_i \omega_i^2}{2} \quad (2)$$

where m_i is the mass of the ith segment, $v_{i,com}$ is the linear velocity of the center of mass of the ith segment relative to the COM, I_i is the moment of inertia, and ω_i is the angular velocity of the ith segment around its center of mass.

EMG activity and bilateral activation. The raw EMG signals were high-pass filtered (30 Hz) and then rectified and low-pass filtered with a zero-lag third-order Butterworth filter (10 Hz) to obtain the EMG envelopes. To reduce residual baseline noise, which appears as offsets in these envelopes, we subtracted the minimum signal from each envelope (Cappellini et al. 2016; La Scaleia et al. 2014). The timescale was normalized by interpolating individual gait cycles over 400 points (i.e., each 0.25% of the stride). For each subject and for each condition, the average EMG activity was calculated across all gait cycles. To obtain an estimate of the total muscle activity across speeds and slopes, we summed the average EMG activity of all muscles after normalizing them to muscle physiological cross-sectional area (PCSA; Ward et al. 2009).

Neuromuscular control of ipsilateral EMG activities has been previously considered during slope walking (e.g., Janshen et al. 2017; Rozumalski et al. 2017; Saito et al. 2018). In this study, we considered instead the functional implications of bilateral muscle activities. The rationale for the bilateral analysis is that the COM motion results from muscle activities of both legs rather than activities of only one leg. To obtain an estimate of the EMG activity of the left side of the subjects, right average EMG activity was half-cycle shifted, assuming perfect symmetry of bilateral activations (Burnett et al. 2011; Pierotti et al. 1991). Bilateral recording of EMG activities of 15 leg muscles has been previously reported for different locomotor conditions and found to be roughly symmetrical (Cappellini et al. 2010). The activity of the left and right leg muscles was then collapsed within one gait cycle defined for the right leg. The EMG signal from each of the 32 muscles (i.e., 16 measured on right side and 16 projected to estimate left side) was then normalized to its peak value across all conditions for each participant.

Bilateral basic activation patterns were extracted with the nonnegative matrix factorization (NNMF) algorithm (Cappellini et al. 2016; Martino et al. 2015). For every subject, slope, and speed, the average muscle activation profiles were concatenated into an $m \times n$ matrix (**M**), where m indicates the number of muscles (32) and n is the number of time-normalized samples (400). The NNMF algorithm was applied to **M** to identify the underlying basic activation patterns P and the associated weighting coefficients C (Lee and Seung 2001) as follows:

$$\mathbf{M} = P \times C + \mathbf{e} \quad (3)$$

where **e** is the residual error matrix. The algorithm searches for an approximate solution to minimize the root-mean-square error between **M** and $P \times C$. For a given number of motor components (see below), the factorization uses an iterative method starting from randomly chosen initial conditions for P and C (Gizzi et al. 2011; Ivanenko et al. 2005; Sartori et al. 2013). Because the root-mean-square error may have local minima, the best solution was selected out of 100 iterations to find C and P from multiple random starting values. The degree of similarity between basic patterns across subjects was evaluated based on the best-matching scalar product of weighting coefficients normalized to Euclidean norm (Cheung et al. 2005; Martino et al. 2015).

The goodness of the pattern decomposition was assessed in terms of the percentage of variance accounted for (VAF; Torres-Oviedo et al. 2006):

$$VAF = 1 - SSE/TSS \quad (4)$$

where SSE is the sum of squared errors between the experimental and reconstructed excitations and TSS is the total sum of squares after

subtraction of the mean from each EMG envelope (Martino et al. 2015). The number of motor components was an input parameter for the NNMF algorithm and was fixed as 4 (as in our previous study, Dominici et al. 2011), because it accounted for >80% of total variance and adding an additional component increased VAF by <5% (see RESULTS).

Spinal maps. To characterize the spatiotemporal patterns of the spinal motor output, the bilateral average EMG activities were mapped onto the estimated rostrocaudal location of the MN pools in the human spinal cord from the L_2 to S_2 segments based on Kendall's myotomal charts as in Ivanenko et al. (2006a, 2013b). In brief, the maps were constructed by adding up the contributions of each muscle to the total activity at each spinal segment. The motor output pattern of each spinal segment S_j was estimated according to the following equation (La Scaleia et al. 2014):

$$S_j = \frac{\sum_{i=1}^{m_j} \left(\frac{k_{ji}}{n_i} \right) \times \mathrm{EMG}_i}{\sum_{i=1}^{m_j} \left(\frac{k_{ji}}{n_i} \right)} \times \mathrm{MN}_j \quad (5)$$

where EMG_i represents the subject-specific envelope of muscle activity, k_{ji} is a weighting coefficient for the ith muscle ($k_{ji} = 1$, 0.5, or 0 if the jth spinal level is a major, minor, or no source of MN for this muscle, respectively, according to Kendall's charts), m_j is the number of muscles innervated by the jth spinal segment, and n_i is the total number of spinal levels that innervate the ith muscle, again accounting for major and minor sources. To account for size differences in MN pools at each spinal level, this fractional activity value was then multiplied by the segment-specific number of MNs (MN_j), taken from Tomlinson and Irving (1977).

To obtain the averaged (across subjects) spinal maps at each speed and slope, we calculated the spinal motor output for each subject based on averaged normalized EMG patterns and then averaged spinal maps across subjects. To compute the relative activation of the lumbar and sacral segments in each walking condition, we averaged the motor output patterns over the gait cycle in the upper part of the lumbar (sum of the activity from L_2 to L_4) and the sacral (sum of activity from S_1 to S_2) segments. Because of its intermediate position, spinal segment L_5 has not been taken into account.

Statistics

Data were grouped into speed-slope classes. For each variable studied, to obtain one value per subject in each speed-slope class, the data measured on each stride of a given trial were averaged. The mean and standard deviation of the population were then computed in each speed-slope class (grand mean). Similarly, the curves obtained on each stride of a given subject in a speed-slope class were averaged (mean curve). Then, the mean curves of all the subjects were averaged in each speed-slope class (ensemble averaged). After checking for normality of data distribution, the variables were analyzed across all conditions by using a repeated-measures ANOVA with post hoc Bonferroni correction to assess the difference between conditions (PASW Statistics 19, SPSS, IBM). An α threshold of 0.05 was used throughout to assess statistical significance.

Both for temporal basic activation patterns and weighting coefficient, similarities between level and slope walking at each speed of progression were assessed by measuring the scalar product between data of individual subjects walking on slope and the average data across subjects walking on the level. Similarities between level and slope walking at different speeds were assessed by correlating the time curves of basic muscle activation pattern, of COM and peripheral power, and of lumbar and sacral segment motor output during walking on a slope with the time curves during walking on the level. Therefore, we measured the Pearson correlation between curves of individual subjects walking on a slope and the average curve (across subjects) obtained during level walking. To average the individual correlations across subjects, we averaged the Fisher's z-transformed r and back-transformed the average z value.

RESULTS

Gait Parameters and Mechanical Power

The step frequency f increases with speed (ANOVA; $F = 605.7$, $P < 0.001$) but is not significantly affected by the slope of the terrain (Bonferroni post hoc; $P > 0.344$), except at $-9°$, where f is slightly greater than on the level (Fig. 1*B*), especially at slow walking speeds. These results are in accordance with Kawamura et al. (1991) and Sun et al. (1996). The relative duration of stance and swing phases is also affected by the speed of progression since t_{DC} decreases with increasing speed (ANOVA; $F = 204.3$, $P < 0.001$). t_{DC} is not affected by the slope of the terrain (Bonferroni post hoc; $P > 0.062$), except at $-9°$, where t_{DC} is slightly shorter than on the level, especially at slow walking speed. The time (t_v) between FC and the minimum of the vertical component of velocity of the COM changes with gait speed (ANOVA; $F = 40.3$, $P < 0.001$) but also with slope (ANOVA; $F = 189.6$, $P < 0.001$). At slow speed, t_v occurs around FC at all slopes. As speed increases, t_v occurs later on negative slopes and earlier both on the level and on positive slopes.

The $\dot{E}_{per}$ curves are highly affected by the speed of progression but are similar across slopes (Fig. 1*A*): the correlation coefficient (r^2) of the time course between $\dot{E}_{per}$ on slopes and $\dot{E}_{per}$ on the level is 0.88 ± 0.07 at 0.83 m/s, 0.93 ± 0.05 at 1.39 m/s, and 0.93 ± 0.07 at 1.94 m/s. The $\dot{W}_{com}$ curves are highly affected by both speeds and slopes: the correlation coefficient between $\dot{W}_{com}$ curves on slopes and $\dot{W}_{com}$ on the level is 0.38 ± 0.44 at the slowest speed and increases up to 0.83 ± 0.17 at the highest speed (Fig. 1*A*).

The modifications of the gait dynamics with slope are thus mainly linked to modifications of $\dot{W}_{com}$. In level and downhill walking, the $\dot{W}_{com}$-time curves display one peak of negative power ($\dot{W}^-$) occurring ~10% after FC. At low walking speeds, the magnitude of this peak is slightly greater when walking downhill than when walking on the level. When speed increases, the magnitude of this peak changes ($F_{3,215} = 236.09$, $P < 0.001$) at a faster rate in downhill walking than on the level. During level and uphill walking, the $\dot{W}_{com}$-time curves display two peaks of positive power.

At all slopes, the magnitude of $\dot{W}_1^+$ is greater than the magnitude of $\dot{W}_2^+$. When walking uphill at slow speeds, the magnitude of these two peaks is greater than on the level ($\dot{W}_1^+$ $F_{3,215} = 284.46$, $P < 0.001$ and $\dot{W}_2^+$ $F_{3,215} = 171.44$, $P < 0.001$). When speed increases, these two peaks increase ($F_{6,215} = 218.59$ and $F_{6,215} = 161.01$, $P < 0.001$) at a faster rate in uphill walking than on the level ($F_{6,215} = 102.81$, $P < 0.001$). When walking downhill, both $\dot{W}_1^+$ and $\dot{W}_2^+$ decrease with increasing slope. Note that on steep negative slopes $\dot{W}_2^+$ tends to disappear.

EMG Activity

Figure 2*A* illustrates the ensemble-averaged EMG envelopes when walking on the level and on a +9° and a −9° slope.

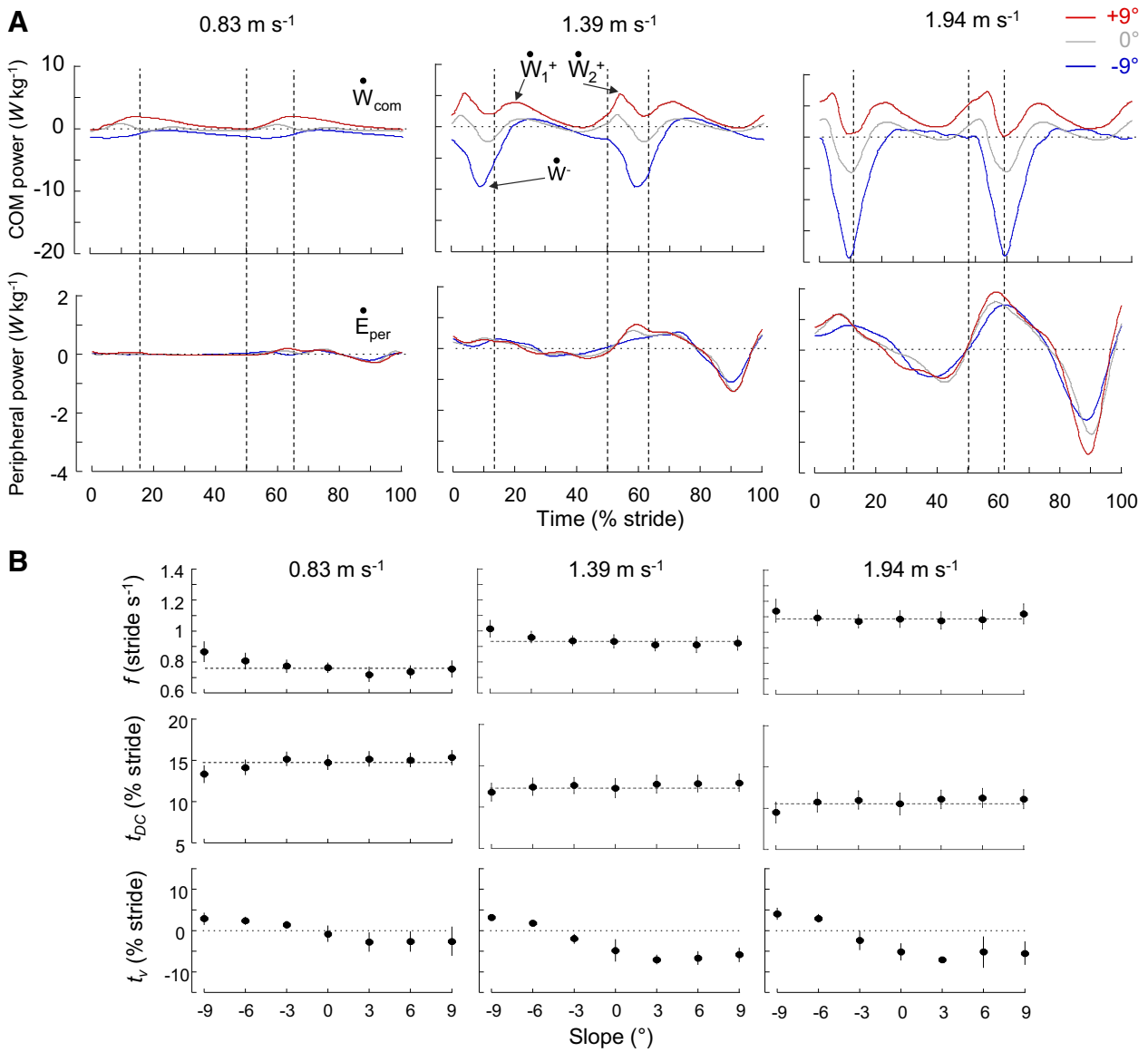

Fig. 1. Center of body mass (COM) and peripheral power and stride parameters during walking at 0.83, 1.39, and 1.94 m/s on different slopes. *A*: ensemble-averaged time curves (see METHODS) of the mass-specific COM (*top*) and peripheral (*bottom*) powers (also referred to as external and internal power) during walking at 0.83, 1.39, and 1.94 m/s on a −9°, 0°, or +9° slope. Time is expressed as % of stride period (0% and 100% of stride correspond to the right foot contact). Vertical dashed lines correspond to foot contact (50% of stride corresponds to the left foot contact) and toe-off. Note that at a given speed curves of the peripheral power are similar across slopes, whereas curves of the COM power change drastically with slope. $\dot{W}_{com}$, COM power; $\dot{W}^{+}_{com}$, positive portion; $\dot{W}^{-}_{com}$, negative portion; $\dot{E}_{per}$, peripheral power. *B*: gait parameters (means ± SD) as a function of slope in the 3 speed-classes. Gait parameters are, from *top* to *bottom*: stride frequency (*f*), relative duration of the double contact phase (t_{DC}), and the time between touchdown and the minimum vertical velocity of the COM (t_v). t_{DC} and t_v are expressed in % of stride period. The horizontal dashed lines correspond to level walking. Symbols and bars represent the grand mean and the SD (when the length of the bar exceeds the size of the symbol).

EMGs are visually consistent with those reported in the literature for level walking (Ivanenko et al. 2006a; Winter 1991) and inclined walking (Lange et al. 1996; Sun et al. 1996).

In all muscles, the mean EMG amplitude changes with the speed of progression (ANOVA; $F_{6,355} > 3.7$, $P < 0.002$) and with the slope of the terrain (ANOVA; $F_{6,355} > 11.9$, $P < 0.001$). When speed increases, muscle activities increase. By contrast, the changes across positive or negative slopes are different: for +9° uphill walking the average EMG amplitude of all muscles over the gait cycle is increased compared with level walking (Bonferroni post hoc ;$P < 0.001$), whereas on a −9° slope the average amplitude of some EMGs is reduced with slope (ADD, ST, TA, MG, LG, PERL; Bonferroni post hoc; $P < 0.032$) and the amplitude of other EMGs is increased (TFL, VM, VL, RF; Bonferroni post hoc; $P < 0.001$). As a result, the summed average EMG activity of all muscles normalized to the cross-sectional area have a minimum at a slope ranging between −3° at slow speeds and −6° at high speeds (Fig. 2*B*).

When walking on a slope, there are also deviations from EMG bursting patterns observed during level walking. Indeed, additional bursts of activity appear in uphill and downhill walking. For instance, an additional burst of activity appears in the distal extensors (MG, LG, SOL, PERL)

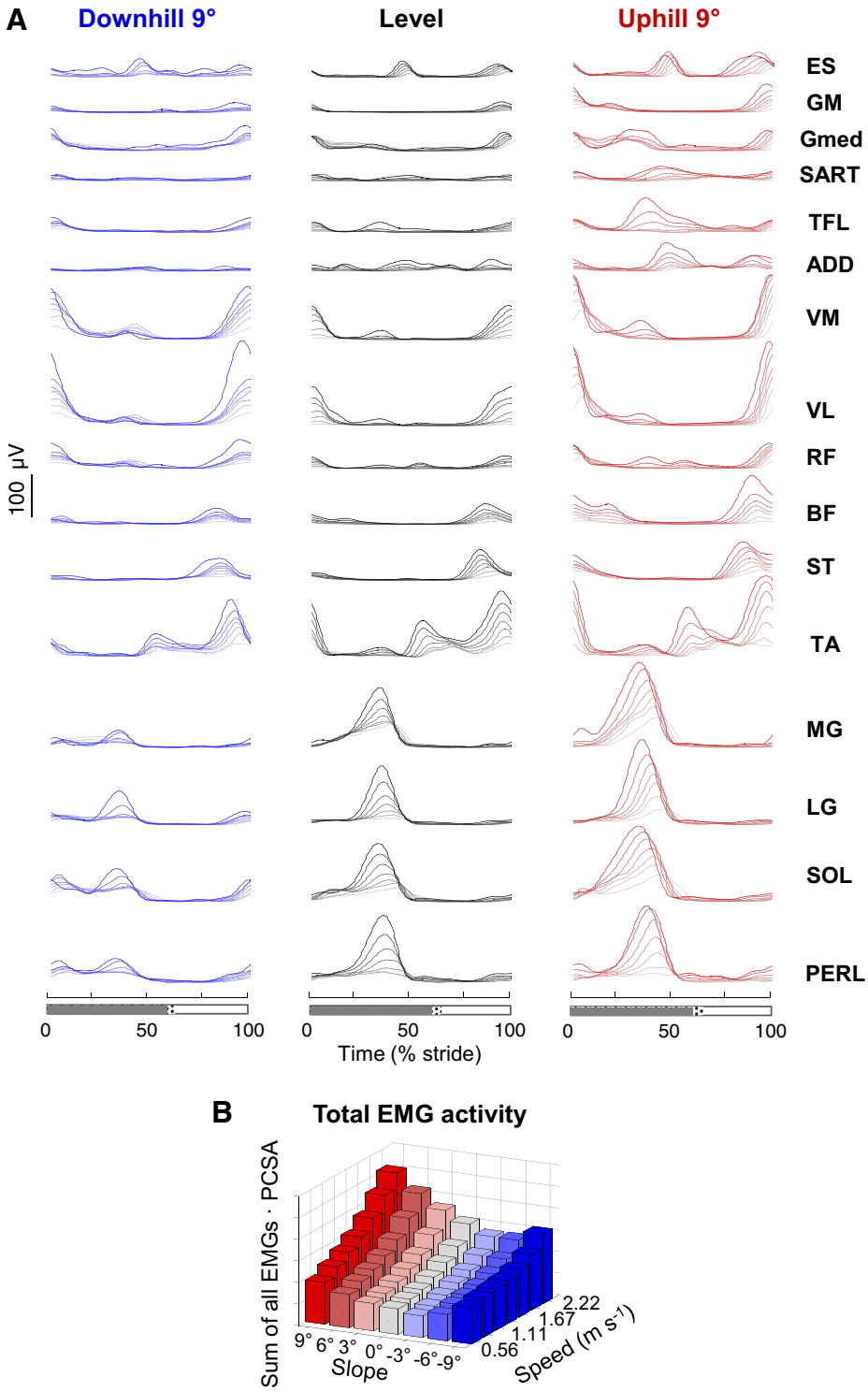

Fig. 2. Ensemble-averaged electromyogram (EMG) patterns during walking at different speeds and slopes. *A*: ensemble-averaged EMG patterns during walking at different speeds (color intensity increases with speed) on a −9° slope (*left*), on the level (*center*), and on a +9° slope (*right*). ES, erector spinae; GM, gluteus maximus; Gmed, gluteus medius; SART, sartorius; TFL, tensor fascia latae; ADD, adductor longus; VM, vastus medialis; VL, vastus lateralis; RF, rectus femoris; BF, biceps femoris; ST, semitendinous; TA, tibialis anterior; MG, gastrocnemius medialis; LG, lateral gastrocnemius; SOL, soleus; PERL, peroneus longus. Stance (gray bar) and swing (white bar) are shown at *bottom*. As the relative duration of stance varied with speed, a hatched region also indicates an amount of variability in the stance phase duration across speeds. *B*: total EMG activity normalized to the physiological cross-sectional area (PCSA) of muscles (Ward et al. 2009) at all speeds and slopes. Note a minimum between −3° and −6° slope depending on the walking speed.

at the onset of stance at negative slopes, which is normally absent during level walking.

Bilateral Basic Activation Patterns

Analysis of dimensionality with the NNMF method shows that bilateral EMG activity changes during slope walking are captured by a small number of motor modules (Fig. 3). The percent total VAF by four basic patterns is equal to 85.1 ± 4.9% (mean ± SD) (Fig. 3*A*). Adding an additional component increased VAF by only 4.2 ± 2.0%. A small but significant effect of speed is observed on the VAF ($F_{6,360} = 3.8$, $P = 0.001$): the VAF decreases with increasing speed, from 0.56 to 2.22 m/s. Note that the VAF was greater in downhill walking than on the level or uphill walking.

Because the timing of four main activity peaks during walking is temporally synchronized on opposite sides of the body, two patterns (*P3* and *P4*) are phase shifted by one half-cycle from the other two (*P1* and *P2*). Accordingly, the

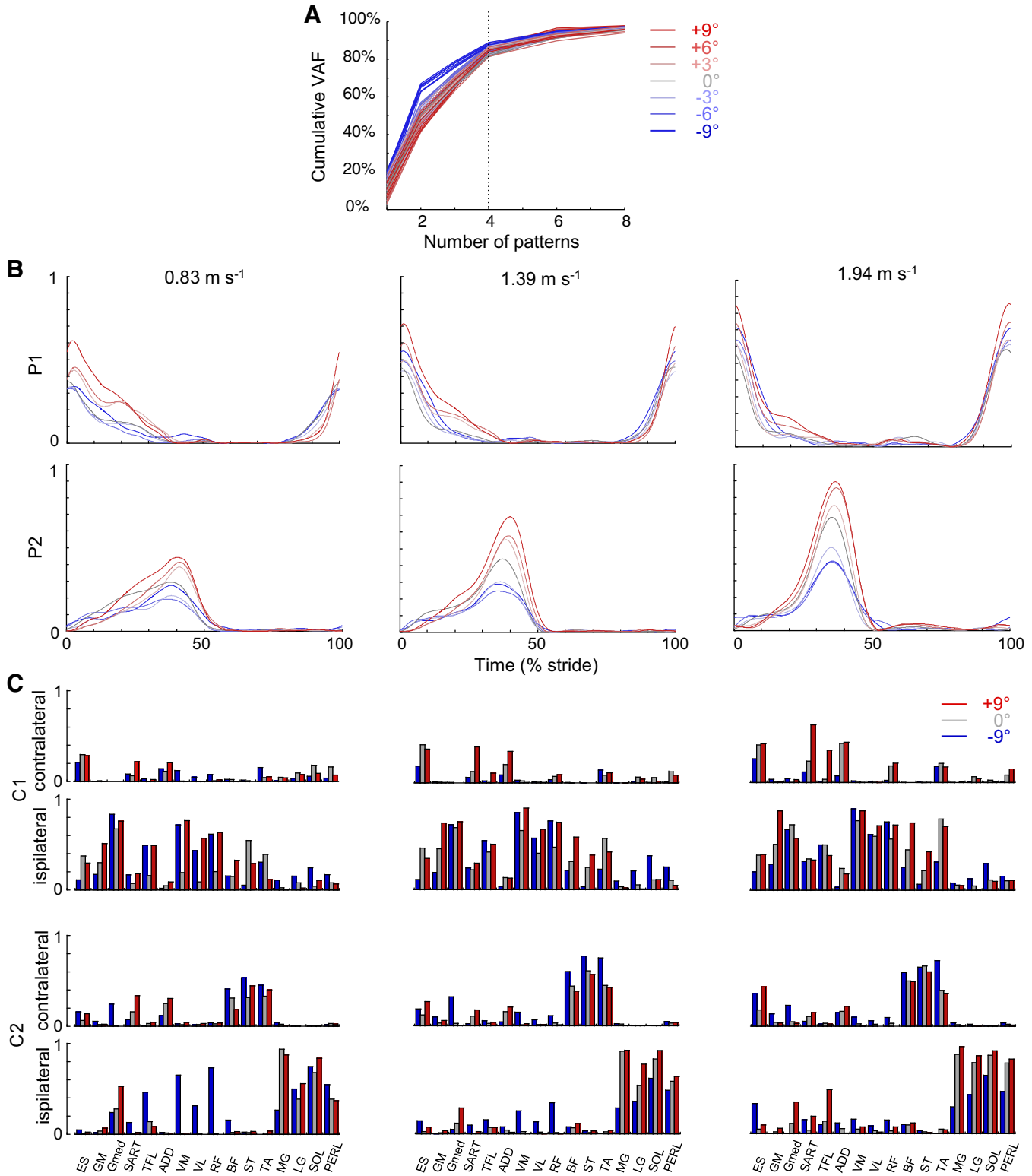

Fig. 3. Bilateral basic muscle activation patterns assessed by nonnegative matrix factorization (NNMF). *A*: cumulative % of variance accounted for (VAF) explained by basic electromyogram (EMG) patterns at all speeds and slopes. *B*: basic activation patterns during walking at 0.83, 1.39, and 1.94 m/s on different slopes. Each curve represents the ensemble-averaged pattern for a specific slope. The basic patterns are named in a "chronological" order (*P1* appears around foot contact, whereas *P2* appears at the end of single stance, etc.). Since *P3* and *P4* were half-cycle-shifted copies of *P1* and *P2*, we illustrate only *P1* and *P2* (accordingly, the associated weighting coefficients of *P1* and *P2* are the same as for *P3* and *P4* but reversed for the ipsilateral and contralateral legs). *C*: corresponding group mean weights (synergies; *C1* and *C2*) for ipsilateral and contralateral leg muscles in −9° downhill, level, and +9° uphill walking. The gait cycle starts with the right foot contact, whereas the NNMF analysis was performed for bilateral EMG envelopes, so that weights for the ipsilateral and contralateral leg muscles are different. ES, erector spinae; GM, gluteus maximus; Gmed, gluteus medius; SART, sartorius; TFL, tensor fascia latae; ADD, adductor longus; VM, vastus medialis; VL, vastus lateralis; RF, rectus femoris; BF, biceps femoris; ST, semitendinous; TA, tibialis anterior; MG, gastrocnemius medialis; LG, lateral gastrocnemius; SOL, soleus; PERL, peroneus longus.

associated weighting coefficients of *P1* and *P2* are the same as for *P3* and *P4* but reversed for the ipsilateral and contralateral legs. Therefore, only the basic activation patterns *P1* and *P2* and the corresponding weightings (muscle synergies) are reported in Fig. 3, *B* and *C*. Although both slope and speed affect the associated weighting coefficients (Fig. 3*C*), the timing of activity peaks (Fig. 3*B*) is relatively invariant across speeds and slopes: pattern *P1* occurs around FC, whereas pattern *P2* occurs during the second part of single stance. However, the shape and the amplitude of the basic activation patterns (Fig. 3*B*) are modified with speed and slope. The peak magnitude of all basic patterns increases with speed (ANOVA; $F_{6,360} > 75.9$, $P < 0.001$) and on positive slopes compared with on the level (Bonferroni post hoc; $P < 0.037$). On negative slopes, the maximum of *P1* increases whereas the maximum of *P2* decreases compared with on the level (Bonferroni post hoc; $P < 0.001$).

Spinal Maps

Figure 4 presents the average segmental MN output over one gait cycle. Qualitative similarities in temporal profile are observed across speeds and slopes. In particular, two major "spots" of activity are present: the first burst around FC mainly localized on the lumbar segment and the second burst during the second part of single stance mainly localized on the sacral segment.

In contrast to the qualitatively similar temporal characteristics, there are substantial differences in the intensity of spinal activation across slopes. In particular, the most striking feature in the spinal maps is a systematic change in the lumbar and sacral segmental outputs. The mean motor output intensity of the total lumbar (L_2–L_4) and sacral (S_1–S_2) MN activation increases with speed of locomotion (lumbar $F_{6,360} = 80.8$, $P < 0.001$; sacral $F_{6,360} = 67.1$, $P < 0.001$). These intensities are also affected by the slope of the terrain (lumbar $F_{6,360} = 54.4$, $P < 0.001$; sacral $F_{6,360} = 79.5$, $P < 0.001$): compared with the level, the maximal intensity of the lumbar MN activation increases in both positive and negative slopes whereas the maximal intensity of the sacral MN activation increases in uphill walking and slightly decreases in downhill walking. Note that the effect of speed on sacral activity is more marked on a positive than a negative slope ($F_{6,360} = 1.76$, $P < 0.006$).

Correspondence Between Mechanical Power and Spinal Maps

Since $\dot{E}_{per}$ curves are similar across slopes (Fig. 1*A*), the modifications of spinal motor output are mainly related to changes in $\dot{W}_{com}$-time curves. During level walking, the $\dot{W}_{com}$-time curves during each step tend to follow a consistent pattern of fluctuations (Fig. 1*A* and Fig. 5). A phase of negative power ($\dot{W}^-$) presenting a peak ~10% after FC occurs after the collision with the ground. $\dot{W}^-$ is followed by a first phase of positive power ($\dot{W}_1^+$; Fig. 6*C*). The phases $\dot{W}^-$ and $\dot{W}_1^+$ contribute to the vertical redirection of the COM after FC and are designated as the Collision phase. A

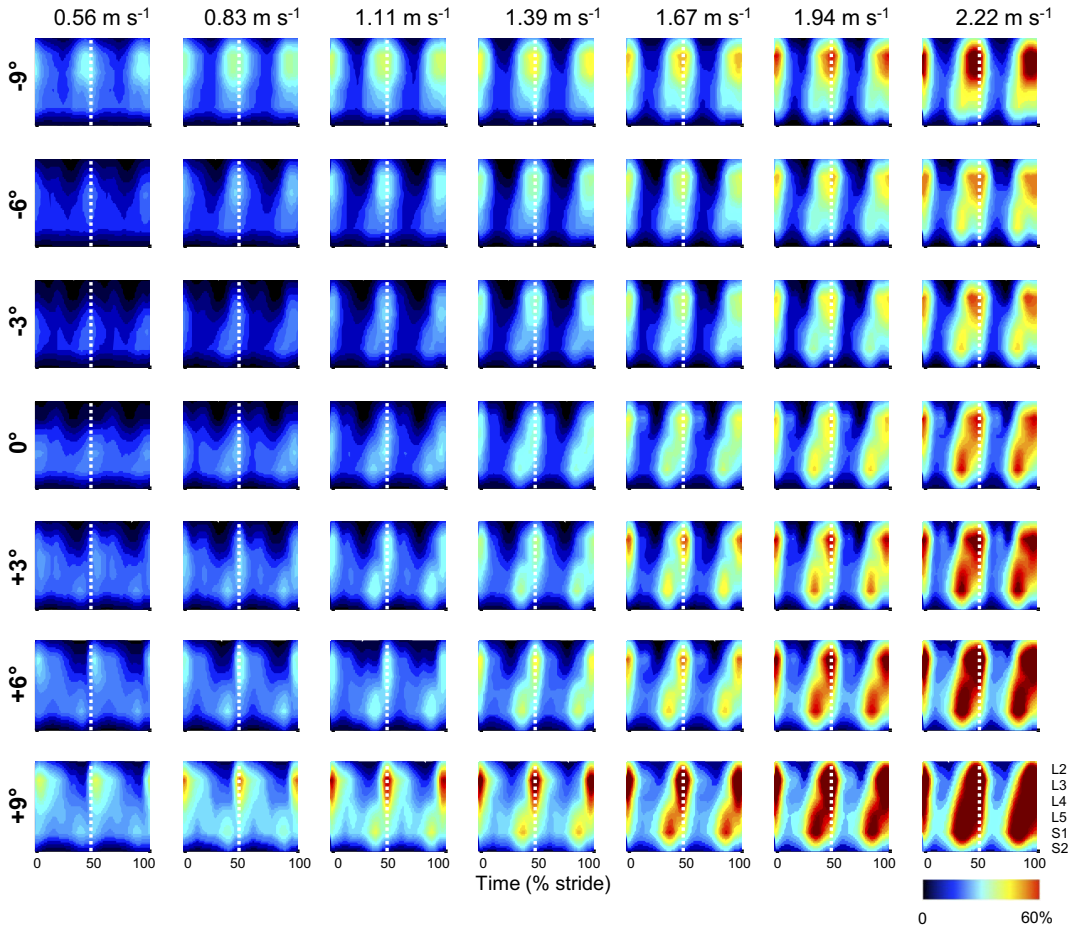

Fig. 4. Bilateral spatiotemporal spinal motor outputs computed from ensemble-averaged electromyograms (EMGs) during walking at different speeds and slopes. Motor output (reported in % of maximal activation) is plotted as a function of gait cycle, the vertical white dotted line corresponding to half (50%) of gait cycle. Note that the intensities of both the lumbar and the sacral segments increase monotonically with speed, but that these intensities change differently on positive and on negative slopes.

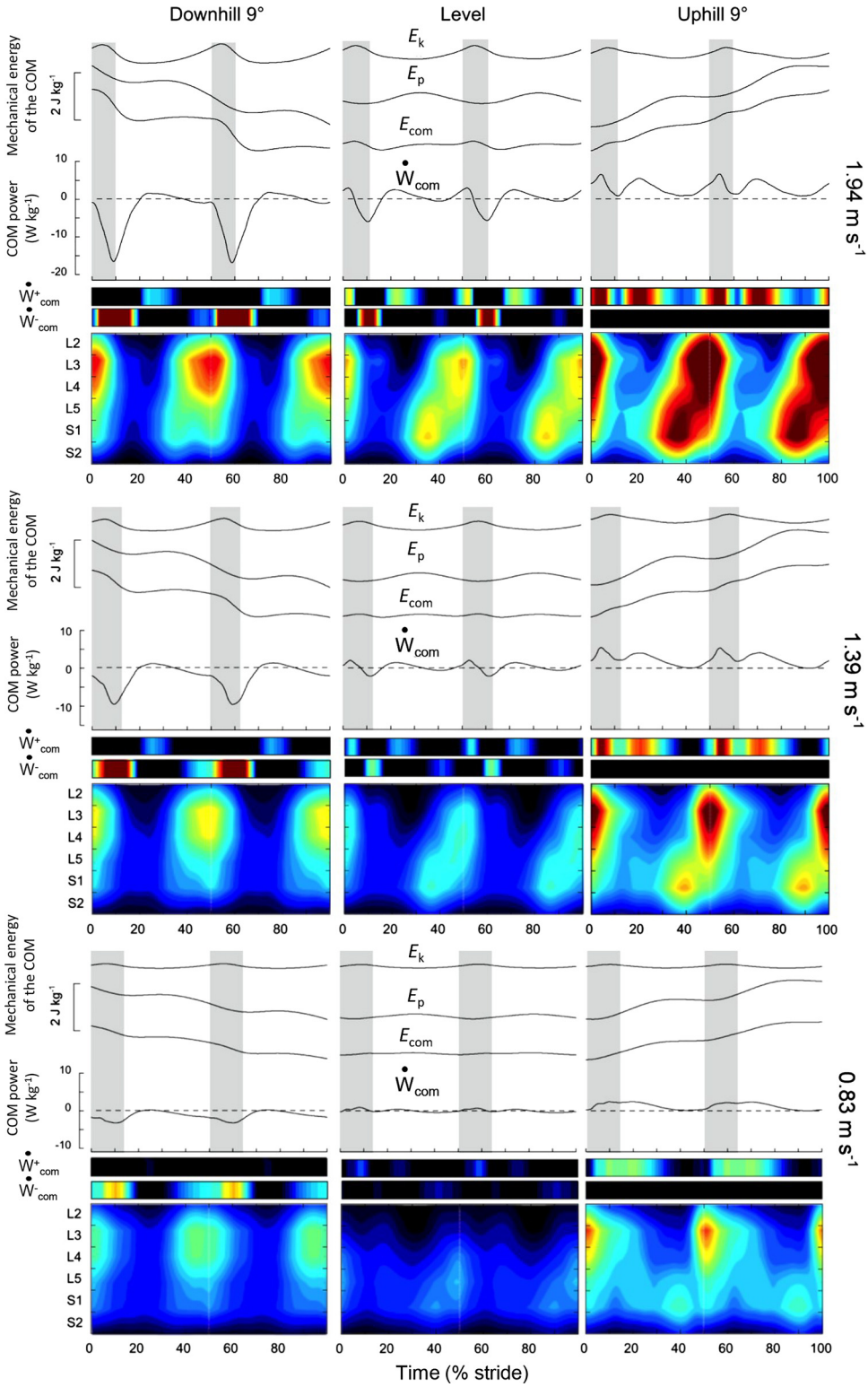

Fig. 5. Mechanical energy of the center of body mass (COM) motion and spinal maps during walking at 0.83, 1.39, and 1.94 m/s on a −9° slope (*left*), on the level (*center*), and on a +9° slope (*right*). *Top*: the ensemble-averaged mass-specific mechanical energy-time curves of the COM during a stride. E_k, the kinetic energy of the COM; E_p, its gravitational potential energy; E_{com}, the total energy of the COM ($E_{com} = E_k + E_p$). *Middle*: the COM power ($\dot{W}_{com}$, black curves) and its positive ($\dot{W}^+_{com}$) and negative ($\dot{W}^-_{com}$) portions (color scale). Gray zones correspond to the double contact periods. *Bottom*: color plots refer to the bilateral spinal maps of motoneuron activity (the same format as in Fig. 4).

second phase of positive power ($\dot{W}^+_2$; Fig. 6*C*) starts at the end of single stance, and its peak occurs close to the bottom of the COM trajectory. This phase accelerates the COM and is designated as the Push-off phase.

We observe a systematic temporal correspondence between the major loci of MN activity and the fluctuations of $\dot{W}_{com}$ (Fig. 5 and Fig. 6). Note that a temporal delay occurs between MN activations and the peaks of $\dot{W}_{com}$. First, there is a temporal correspondence between the MN activity of the lumbar locus and the occurrence of the Collision phase. This first locus is associated with EMG activity in proximal lower limb and ankle dorsiflexor muscles. The lumbar segment activation increases with slopes in both downhill and uphill walking. $\dot{W}^-$ increases on a negative slope,

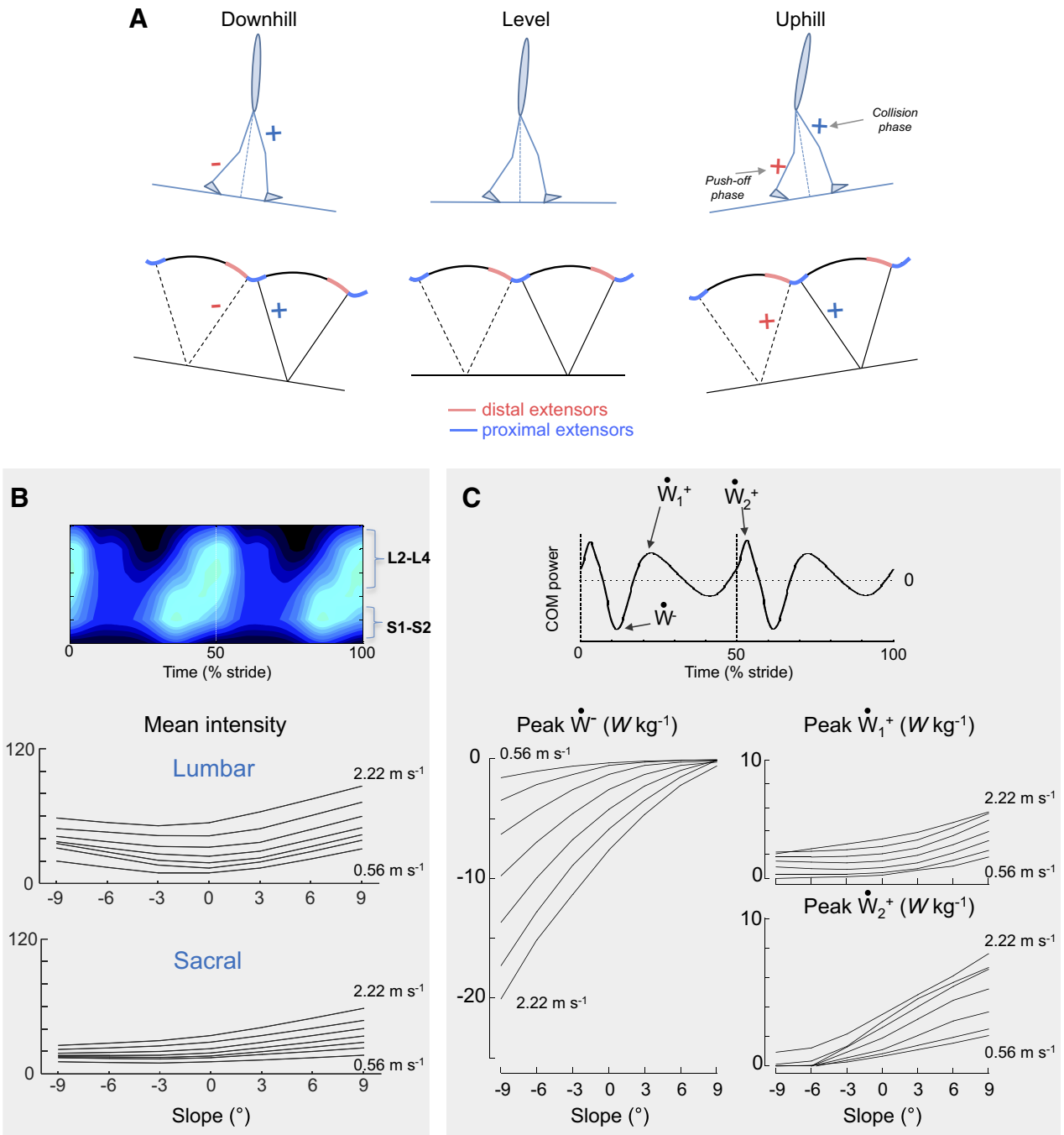

Fig. 6. Differential changes in the lumbar and sacral spinal locomotor output and center of body mass (COM) power. *A*: schematic representation of changes in the proximal and distal extensor muscles with slope. + and − signs mean that the muscular activity increases/decreases compared with level walking. *B*: changes in the mean intensity of the estimated upper lumbar (L_2+L_3+L_4) and sacral (S_1+S_2) segments with walking speed and slope. *C*: changes in the positive ($\dot{W}_1^+$ and $\dot{W}_2^+$) and negative ($\dot{W}^-$) peaks of the COM power with speed and slope. Since there are 2 peaks of $\dot{W}_{com}$ in most conditions (see Figs. 1 and 5), the amplitude of both the first $\dot{W}_1^+$ and second $\dot{W}_2^+$ peaks was evaluated (*right*).

whereas $\dot{W}_1^+$ increases on a positive slope. As a result, there is increasing MN activity in the lumbar locus during the Collision phase. Second, there is a systematic temporal correspondence between the MN activity of the sacral locus and the occurrence of the Push-off phase. When slope changes from −9° to +9°, both the sacral spinal activity and $\dot{W}_2^+$ increase, suggesting monotonic changes in the Push-off phase between a steep negative and a steep positive slope.

Differential Effect of Speed

Changes in the motor pattern due to inclination of the terrain depend on walking speed. Indeed, the correlation between basic activation patterns (*P1* and *P2* and *C1* and *C2*) on a steep slope and the same patterns on the level is smaller at slow than at fast speeds (Fig. 7*A*). The same observation can be made for the lumbar and sacral segment activities (Fig. 7*B*).

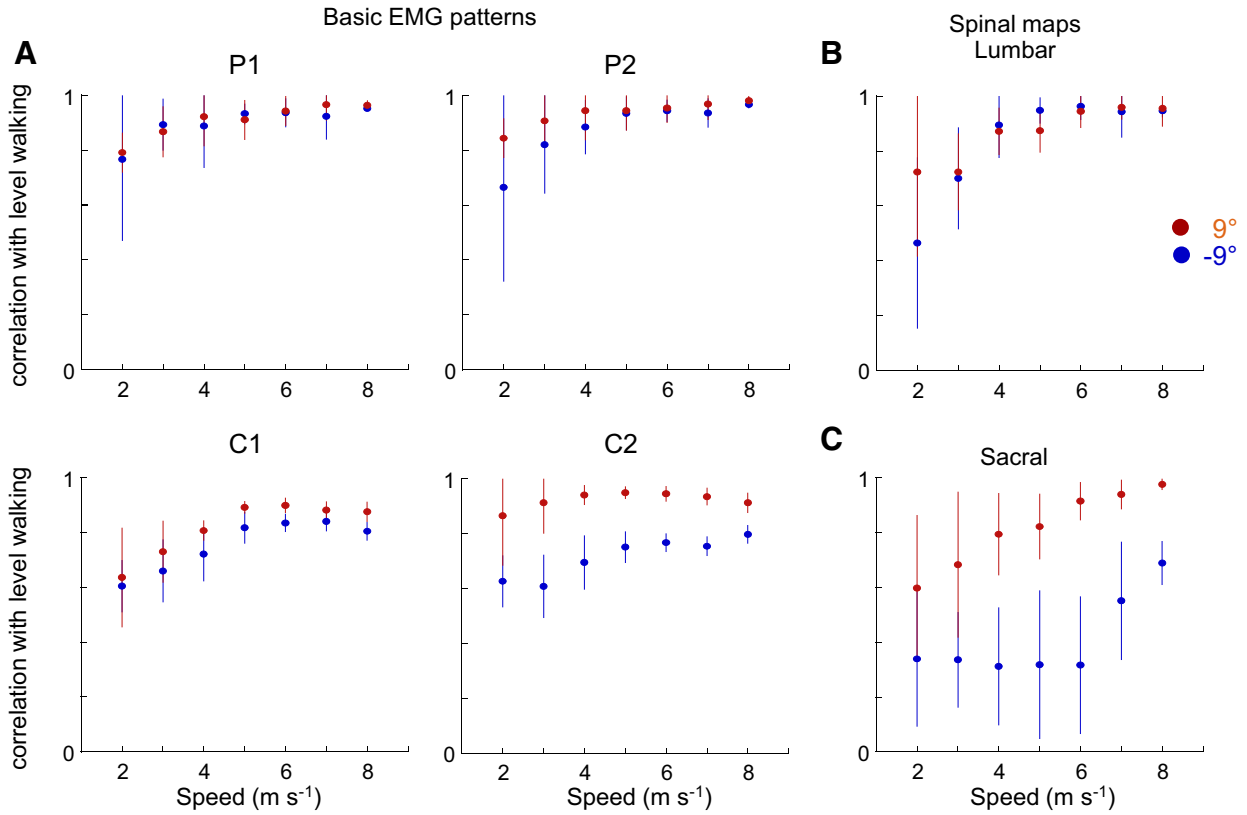

Fig. 7. Differential effect of speed during walking on ±9° slopes. *A*, *top*: correlation between basic muscle activation patterns (*P1* and *P2*) on a slope and basic muscle activation patterns on the level, as a function of speed. *Bottom*: correlation between muscle synergies (*C1* and *C2*) on a slope and muscle synergies on the level. *B*: correlation between lumbar activity (L_2+L_3+L_4) when walking on a slope and lumbar activity when walking on the level. *C*: correlation between sacral activity (S_1+S_2) when walking on a slope and sacral activity when walking on the level. Patterns, synergies, and lumbar and sacral activities from individual subjects walking on a slope are correlated with the grand mean of these variables obtained during level walking. Points and bars represent the mean correlation ± SD of the correlation coefficients (see METHODS).

DISCUSSION

In this study, we examined neuromechanical relationships between lower limb muscle activity, associated spinal motor pool activation, and COM kinetics in humans walking at different speeds on different slopes. Spinal maps (Fig. 4 and Fig. 5) showed four major loci of activity associated with the major kinetic events of the Collision and Push-off phases (Fig. 5 and Fig. 6). Furthermore, the results supported our expectation that walking on negative and positive slopes at different speeds is characterized by a different involvement of the lumbar and sacral motor pools (Fig. 6). Statistical analysis of bilateral muscle activity patterns confirmed a similar temporal organization of the major bursts of activity but showed differential changes in the amplitude of basic activation patterns as a function of speed and slope (Fig. 3). Below, we discuss the changes of the segmental spinal motor output in relation to power production, supporting the idea that multiple generators of locomotor activity are differentially activated as a function of speed and slope.

EMG Patterns and General Biomechanical Characteristics of Walking on Slopes

During walking, muscles consume metabolic energy for positive and negative work related to raising/lowering and accelerating/decelerating the body's center of mass and limb segments during each stride (Minetti et al. 1993). When walking on a slope, the COM dynamics undergo significant modifications (Dewolf et al. 2017), mainly linked to modification of COM power due to changes in the COM gravitational potential energy. These different biomechanical demands on slopes require changes in the activity from lower limb muscles. In line with several previous studies in both humans and quadrupeds (Carlson-Kuhta et al. 1998; Hunter et al. 2010; Lay et al. 2007; Pickle et al. 2016; Smith et al. 1998), slope-related changes of EMG activity are highly nonlinear, in contrast to the quasi-linear changes with speed (Fig. 2*A*). For instance, during uphill walking, the mean activity of all muscles increases. Compared with uphill walking, downhill walking is characterized by greater modifications of the motor output: some muscles show limited changes, whereas others systematically increase or decrease their activity when the slope becomes steeper (Fig. 2*A*).

Because of the force-velocity relationship, the muscle force produced for a given activation as well as the corresponding metabolic cost depend on the mode of contraction (concentric or eccentric). Furthermore, subjects' individual differences in PCSA and in thickness of subcutaneous adipose tissue have not been taken into account in this study. Therefore, the sum of PCSA-normalized average EMG activity of all muscles should only be considered as a qualitative parameter, particularly when related to energy consumption. Regardless of those limitations, the overall estimated intensity of EMG activity normalized to the cross-sectional area of muscles shows mono-

tonic changes with speed and presents a minimum around a −3 to −6° slope, depending on walking speed (Fig. 2*B*). This slope is close to the metabolic optimum slope of approximately −6° (Hunter et al. 2010; Minetti et al. 1993).

Sequential Activation of Lumbar and Sacral Segments

We previously reported that the segmental spinal motor output in humans reveals temporal similarities for disparate walking behaviors, exhibiting peaks around foot strike (Collision) and foot lift (Push-off) for each lower limb (La Scaleia et al. 2014). Moreover, net spinal motor output contributes to mechanical work, mainly during the step-to-step transition to raise/accelerate the COM (Bianchi et al. 1998). The motor patterns on both sides exhibit bursts of activity around foot liftoff of the trailing limb and touchdown of the leading limb (Ivanenko et al. 2006b; La Scaleia et al. 2014, Olree and Vaughan 1995; MacLellan et al. 2014). Accordingly, basic bilateral muscle activation patterns (Fig. 3) show four major loci of activity: these peaks are synchronized on opposite sides of the body so that two patterns (*P3* and *P4*) are phase shifted by a half-cycle from the other two (*P1* and *P2*). These four basic patterns account for ~85% of the total EMG variance of recorded muscles (Fig. 3*A*); the remaining (~15%) activity is likely related to the natural EMG variability and/or online control of postural/kinematic disturbances and corresponding variability in the sensory feedback. Although this bilateral temporal "program" is rather invariant across speeds and slopes, the shape/amplitude of the basic activation patterns (Fig. 3*B*) and the associated weighting coefficients (Fig. 3*C*) change with speed and slope. In particular, the amplitude of the first basic component *P1* increases in both uphill and downhill walking, whereas the amplitude of *P2* increases during uphill but decreases during downhill walking (Fig. 3).

Slope-related changes in motor patterns were previously discussed in terms of unit burst generators (Grillner 1981) for the control of extensor/flexor muscles of the hip, knee, ankle, or foot (Smith et al. 1998) and of the joint torques (Lay et al. 2007; Pickle et al. 2016). Whereas a comparative analysis of joint powers with the motor pool activation would be meaningful in terms of understanding the contribution of individual joints and muscle groups to the biomechanics of walking on slopes, the lower limb EMG activities are not easily related to joint moments, especially during uphill walking (Lay et al. 2007). Indeed, several muscles are bi- or multiarticular, acting on several joints simultaneously. Some muscles may also generate a noticeable lateral force component (Dostal et al. 1986). Moreover, just because of physics, a torque exerted at one joint may also affect angular motion of dynamically coupled joints of the limb (Ivanenko et al. 2013a; Zajac et al. 2003).

The novelty of our study consists in an integrative approach to evaluation of the bilateral spatiotemporal organization of the spinal motor output linked to specific kinetic events. Indeed, both stance- and swing-related muscle activities contribute to the spinal motor output (Ivanenko et al. 2008; Marsh et al. 2004). When multimuscle EMG activity is mapped onto the rostrocaudal location of the MN pools, the bilateral spinal maps show four major loci of activity at all slopes and speeds (Fig. 4 and Fig. 5). The most striking feature in the spinal maps is a systematic change in the lumbar and sacral segmental output (Fig. 4). Figure 6*A* schematically summarizes the main findings. Although the overall activity of sacral motor pools decreases on negative slopes and increases on positive slopes, the lumbar motor pools monotonically increase their engagement at all slopes with regard to level walking.

Relationship Between Spinal Motor Pool Activation and Biomechanics of Bipedal Gait

Peripheral power (also referred to as internal power) to move the limbs relative to the COM is rather independent of slope (Minetti et al. 1993; Fig. 1*A*) whereas COM power (also referred to as external power) accounts for most differences in the energetics of walking on slopes (Fig. 1*A*). Therefore, it is not surprising that the loci of MN activity precede the major peaks in the COM power (Fig. 5). Some temporal delays between muscle power and activation should be expected given the electromechanical delays, elastic energy storage, dynamic coupling, and velocity dependence of muscle-tendon unit functioning plus limb inertia. However, when analyzing both the biomechanical and neurophysiological aspects of gait, our findings point toward the link between segmental motor pool activation and the mechanics of bipedal gait, which presumably reflects the functional grouping of spinal MNs adopted during evolution (Jessell et al. 2011).

On the whole, there are monotonic changes in the sacral spinal activity and in the magnitude of the second peak of positive power ($\dot{W}_2^+$). This Push-off phase mainly corresponds to the peak of positive ankle joint power of the trailing limb at the end of stance (Franz and Kram 2014; Lay et al. 2007; Yang et al. 2019) to accelerate the COM and swing limbs (e.g., Zelik and Adamczyk 2016). Push-off before contralateral limb foot strike may reduce the energy lost because of collision with the ground and in turn the metabolic cost of walking (Kuo 2001). On positive slopes, the sacral spinal activity and $\dot{W}_2^+$ increase and t_v (i.e., the time at which V_v is minimal) appears earlier (Fig. 1*B*). Similar increase is also observed in the amplitude of the second basic bilateral activation pattern *P2* (Fig. 3*B*). *P2* involves primarily the ankle dorsiflexor and knee flexor of the leading limb and the ankle plantar flexors of the trailing limb (Fig. 3*C*), which is related to the greater ankle joint power observed at the end of stance (Lay et al. 2006, 2007; Pickle et al. 2016; Yang et al. 2019). On negative slopes, the decrease in the distal extensor muscle activity results in a decrease in the sacral spinal activity and in the amplitude of P2 (Fig. 3*B*). Furthermore, $\dot{W}_2^+$ tends to disappear, which is related to the reduction of the positive ankle joint power of the trailing limb at the end of stance (Lay et al. 2006, 2007; Pickle et al. 2016; Yang et al. 2019). As a result, t_v occurs after FC (Fig. 1*B*) and a greater collision with the ground occurs at FC.

In the lumbar segment, the MN activation increases when the slope becomes steeper (Fig. 6*B*). This activity is associated with a peak of negative power $\dot{W}^-$ followed by the first peak of positive power $\dot{W}_1^+$. In uphill walking, the lumbar spinal activity increases and is associated with an increase in the amplitude of the first basic bilateral activation pattern *P1*, involving primarily hip and knee extensors of the leading limb and ankle dorsiflexors of the trailing limb (Fig. 3*B*). The positive power $\dot{W}_1^+$ during the Collision phase also increases to complete the vertical lift and corresponds essentially to greater

peaks of positive hip and knee joint power of the leading limb at early stance (Franz and Kram 2014; Lay et al. 2006, 2007). In downhill walking, the lumbar spinal activity and the amplitude of *P1* increase and are associated with an increase in W^- during the Collision phase. This negative power is mainly done to decelerate and lower the COM, via a greater peak of negative knee joint power of the leading limb (Lay et al. 2006, 2007; Pickle et al. 2016) and via soft tissue deformations (Honert and Zelik 2019; Zelik and Kuo 2010).

A comparison of different human gaits and developmental considerations further highlights the link between global biomechanical parameters, such as COM dynamics, and functional spinal cord topography. In neonate stepping, sequential activation of spinal segments and bursts of activity around touchdown and foot liftoff are not yet developed and both lumbar and sacral motor pools are simultaneously activated during midstance (Ivanenko et al. 2013b). In addition, neonates cannot develop enough COM positive and negative power (Dominici et al. 2011; Forssberg 1985), and forward progression needs to be accomplished by the experimenter or by using a moving treadmill belt. In adults, the rostrocaudal displacements of the center of bilateral MN activity mirror the changes in the mechanical energy of the COM motion during both forward and backward walking, as well as in running (Cappellini et al. 2010). During walking on the slippery surface, the shear forces were reduced and the center of MN activity and the kinetic energy oscillations decreased in parallel (Cappellini et al. 2010).

The present results corroborate recent findings about the specialization of neuronal networks located at different segments of the spinal cord for performing specific locomotor tasks. For example, Minassian et al. (2017) suggest that the lumbar pattern generator activity may represent the major oscillator "pacemaker," and Cazalets and Bertrand (2000) show that the sacral generator may play a more subordinate role, e.g., for adaptation to specific foot-support interactions (Selionov et al. 2009). Moreover, the locomotor neural networks do not seem to fully overlap at the same spinal segments for different locomotor tasks. For instance, in the cat the neuronal networks responsible for forward locomotion are distributed broadly in the lumbosacral segments, whereas networks generating backward locomotion are limited to the caudal part of the spinal cord (Merkulyeva et al. 2018). In addition, substantial reorganization of spinal locomotor networks is observed when moving on slopes (Carlson-Kuhta et al. 1998; Smith et al. 1998), somewhat similar to that observed in human. Indeed, based on anatomical models of the organization of the MN pools within the cat lumbar enlargement (Yakovenko et al. 2002), in downhill walking the modifications of stance-related muscle activities suggest that the motor output of the lower lumbar and sacral segments is reduced whereas that of the upper lumbar segment is increased. In uphill walking, the activities of stance-related muscles increase, suggesting an increase of the upper and lower lumbar segments. Furthermore, when comparing slow and fast speeds of progression, there is no simple scaling of MN and interneuron activity but involvement of rather different neural circuits. This was demonstrated in a variety of animal species (Bellardita and Kiehn 2015; McLean et al. 2008; Yokoyama et al. 2017). Here we observed that, with regard to level walking, modification of basic activation patterns and spinal motor output to slopes is greater at slow speeds than at high speeds (Fig. 7). This is consistent with different telescopic limb behavior on slopes at slow and fast speeds of progression (Dewolf et al. 2018).

Limitations of Study

There are several assumptions implicit in our methods. First, the rectified EMG does not provide a direct measure of the net firing of MNs in the spinal cord (Martinez-Valdes et al. 2018). However, this estimate is reasonable because mean EMG tends to increase fairly linearly with the net motor unit firing rate (Day and Hulliger 2001). Second, we do not take into account some minor interindividual anatomical variability in the spinal maps of MN that has been documented previously (Stewart 1992). Indeed, we used anatomical charts of MN localization in the lumbosacral cord derived from the literature (Kendall et al. 2005) to estimate spatiotemporal maps of activation, since we had no direct estimates of MN localization in our subjects. However, using electrical epidural stimulation of the lumbosacral cord with selective engagement of specific dorsal roots and the corresponding myotomes, Wagner et al. (2018) have recently confirmed Kendall's charts in spinal cord-injured patients undergoing rehabilitation. Third, our analysis focuses on consistent and reproducible patterns of muscle activation across various steps; the averaging procedure addresses that issue. Another limitation is that we recorded only a subset of muscles, whereas each lower limb contains $>$50 muscles and most of them are active during walking (Ivanenko et al. 2006a; La Scaleia et al. 2014; Zelik et al. 2015). Nevertheless, although including more muscles may affect the analysis of muscle synergies (Zelik et al. 2014), it is worth noting that the recorded set of muscles constitutes a large part of the total cross-sectional area of lower limb muscles (Ward et al. 2009). Furthermore, the reconstruction of the spinal motor output from multimuscle EMG recordings is relatively insensitive to the subset of muscles analyzed, provided that the key muscles that we studied here are included (La Scaleia et al. 2014). In particular, the major part of MN activity is organized in bursts (Fig. 4) with tightly coupled phasing in all spinal segments and across the midline (Ivanenko et al. 2006a; Kiehn 2016).

Despite these limitations, our results show changes in the spinal motor output when walking at different slopes and speeds. A striking feature of walking on slopes is the differential involvement of the lumbar and sacral motor pools in relation to changes in the mechanical demand. Such investigations of spatiotemporal patterns of spinal cord activations and their dependence on the walking environment may also have important clinical implications. For instance, differential spinal cord segment stimulation (epidural or transcutaneous) is a promising tool to restore the functioning of the spinal pattern generation circuitry in both animals (Capogrosso et al. 2016; Wenger et al. 2016) and humans (Angeli et al. 2018; Gill et al. 2018; Solopova et al. 2017; Wagner et al. 2018), and such stimulation techniques should take into account differential activation of spinal segments to selectively drive neuroprostheses depending on walking conditions, such as changes in slope.

GRANTS

This study was funded by the Université catholique de Louvain, the Fonds de la Recherche Scientifique (Belgium), the Italian Ministry of Health (IRCCS Fondazione Santa Lucia Ricerca corrente), the Italian Space Agency (Grant I/006/06/0 and MARS-PRE), the Italian Ministry of University and Research (PRIN Grants 2015HFWRYY_002 and 2017CBF8NJ_005), and the Horizon 2020 Robotics Program (ICT-23-2014 under Grant Agreement 644727-CogIMon).

DISCLOSURES

No conflicts of interest, financial or otherwise, are declared by the authors.

AUTHOR CONTRIBUTIONS

Y.I., K.E.Z., F.L., and P.A.W. conceived and designed research; K.E.Z., F.L., and P.A.W. performed experiments; A.H.D., Y.I., and K.E.Z. analyzed data; A.H.D., Y.I., F.L., and P.A.W. interpreted results of experiments; A.H.D. and Y.I. prepared figures; A.H.D. and Y.I. drafted manuscript; A.H.D., Y.I., K.E.Z., F.L., and P.A.W. edited and revised manuscript; A.H.D., Y.I., K.E.Z., F.L., and P.A.W. approved final version of manuscript.

REFERENCES

Adamczyk PG, Kuo AD. Redirection of center-of-mass velocity during the step-to-step transition of human walking. *J Exp Biol* 212: 2668–2678, 2009. doi:10.1242/jeb.027581.

Allen JL, Franz JR. The motor repertoire of older adult fallers may constrain their response to balance perturbations. *J Neurophysiol* 120: 2368–2378, 2018. doi:10.1152/jn.00302.2018.

Angeli CA, Boakye M, Morton RA, Vogt J, Benton K, Chen Y, Ferreira CK, Harkema SJ. Recovery of over-ground walking after chronic motor complete spinal cord injury. *N Engl J Med* 379: 1244–1250, 2018. doi:10.1056/NEJMoa1803588.

Bellardita C, Kiehn O. Phenotypic characterization of speed-associated gait changes in mice reveals modular organization of locomotor networks. *Curr Biol* 25: 1426–1436, 2015. doi:10.1016/j.cub.2015.04.005.

Bianchi L, Angelini D, Lacquaniti F. Individual characteristics of human walking mechanics. *Pflugers Arch* 436: 343–356, 1998. doi:10.1007/s004240050642.

Brown TG. On the nature of the fundamental activity of the nervous centres; together with an analysis of the conditioning of rhythmic activity in progression, and a theory of the evolution of function in the nervous system. *J Physiol* 48: 18–46, 1914. doi:10.1113/jphysiol.1914.sp001646.

Burnett DR, Campbell-Kyureghyan NH, Cerrito PB, Quesada PM. Symmetry of ground reaction forces and muscle activity in asymptomatic subjects during walking, sit-to-stand, and stand-to-sit tasks. *J Electromyogr Kinesiol* 21: 610–615, 2011. doi:10.1016/j.jelekin.2011.03.006.

Capogrosso M, Milekovic T, Borton D, Wagner F, Moraud EM, Mignardot JB, Buse N, Gandar J, Barraud Q, Xing D, Rey E, Duis S, Jianzhong Y, Ko WK, Li Q, Detemple P, Denison T, Micera S, Bezard E, Bloch J, Courtine G. A brain-spine interface alleviating gait deficits after spinal cord injury in primates. *Nature* 539: 284–288, 2016. doi:10.1038/nature20118.

Cappellini G, Ivanenko YP, Dominici N, Poppele RE, Lacquaniti F. Migration of motor pool activity in the spinal cord reflects body mechanics in human locomotion. *J Neurophysiol* 104: 3064–3073, 2010. doi:10.1152/jn.00318.2010.

Cappellini G, Ivanenko YP, Martino G, MacLellan MJ, Sacco A, Morelli D, Lacquaniti F. Immature spinal locomotor output in children with cerebral palsy. *Front Physiol* 7: 478, 2016. doi:10.3389/fphys.2016.00478.

Carlson-Kuhta P, Trank TV, Smith JL. Forms of forward quadrupedal locomotion. II. A comparison of posture, hindlimb kinematics, and motor patterns for upslope and level walking. *J Neurophysiol* 79: 1687–1701, 1998. doi:10.1152/jn.1998.79.4.1687.

Cavagna GA, Kaneko M. Mechanical work and efficiency in level walking and running. *J Physiol* 268: 467–481, 1977. doi:10.1113/jphysiol.1977.sp011866.

Cavagna GA, Saibene FP, Margaria R. External work in walking. *J Appl Physiol* 18: 1–9, 1963. doi:10.1152/jappl.1963.18.1.1.

Cavagna GA, Thys H, Zamboni A. The sources of external work in level walking and running. *J Physiol* 262: 639–657, 1976. doi:10.1113/jphysiol.1976.sp011613.

Cazalets JR, Bertrand S. Coupling between lumbar and sacral motor networks in the neonatal rat spinal cord. *Eur J Neurosci* 12: 2993–3002, 2000. doi:10.1046/j.1460-9568.2000.00169.x.

Cazalets JR, Borde M, Clarac F. Localization and organization of the central pattern generator for hindlimb locomotion in newborn rat. *J Neurosci* 15: 4943–4951, 1995. doi:10.1523/JNEUROSCI.15-07-04943.1995.

Cheung VC, d'Avella A, Tresch MC, Bizzi E. Central and sensory contributions to the activation and organization of muscle synergies during natural motor behaviors. *J Neurosci* 25: 6419–6434, 2005. doi:10.1523/JNEUROSCI.4904-04.2005.

Chvatal SA, Torres-Oviedo G, Safavynia SA, Ting LH. Common muscle synergies for control of center of mass and force in nonstepping and stepping postural behaviors. *J Neurophysiol* 106: 999–1015, 2011. doi:10.1152/jn.00549.2010.

Coscia M, Monaco V, Martelloni C, Rossi B, Chisari C, Micera S. Muscle synergies and spinal maps are sensitive to the asymmetry induced by a unilateral stroke. *J Neuroeng Rehabil* 12: 39, 2015. doi:10.1186/s12984-015-0031-7.

Cuellar CA, Tapia JA, Juárez V, Quevedo J, Linares P, Martínez L, Manjarrez E. Propagation of sinusoidal electrical waves along the spinal cord during a fictive motor task. *J Neurosci* 29: 798–810, 2009. doi:10.1523/JNEUROSCI.3408-08.2009.

Davis RB 3rd, Õunpuu S, Tyburski D, Gage JR. A gait analysis data collection and reduction technique. *Hum Mov Sci* 10: 575–587, 1991. doi:10.1016/0167-9457(91)90046-Z.

Day SJ, Hulliger M. Experimental simulation of cat electromyogram: evidence for algebraic summation of motor-unit action-potential trains. *J Neurophysiol* 86: 2144–2158, 2001. doi:10.1152/jn.2001.86.5.2144.

de Sèze M, Falgairolle M, Viel S, Assaiante C, Cazalets JR. Sequential activation of axial muscles during different forms of rhythmic behavior in man. *Exp Brain Res* 185: 237–247, 2008. doi:10.1007/s00221-007-1146-2.

Dempster WT, Gaughran GR. Properties of body segments based on size and weight. *Am J Anat* 120: 33–54, 1967. doi:10.1002/aja.1001200104.

Dewitz C, Pimpinella S, Hackel P, Akalin A, Jessell TM, Zampieri N. Nuclear organization in the spinal cord depends on motor neuron lamination orchestrated by catenin and afadin function. *Cell Rep* 22: 1681–1694, 2018. doi:10.1016/j.celrep.2018.01.059.

Dewolf AH, Ivanenko Y, Zelik KE, Lacquaniti F, Willems PA. Kinematic patterns while walking on a slope at different speeds. *J Appl Physiol (1985)* 125: 642–653, 2018. doi:10.1152/japplphysiol.01020.2017.

Dewolf AH, Ivanenko YP, Lacquaniti F, Willems PA. Pendular energy transduction within the step during human walking on slopes at different speeds. *PLoS One* 12: e0186963, 2017. doi:10.1371/journal.pone.0186963.

Dewolf AH, Peñailillo LE, Willems PA. The rebound of the body during uphill and downhill running at different speeds. *J Exp Biol* 219: 2276–2288, 2016. doi:10.1242/jeb.142976.

Dominici N, Ivanenko YP, Cappellini G, d'Avella A, Mondì V, Cicchese M, Fabiano A, Silei T, Di Paolo A, Giannini C, Poppele RE, Lacquaniti F. Locomotor primitives in newborn babies and their development. *Science* 334: 997–999, 2011. doi:10.1126/science.1210617.

Dostal WF, Soderberg GL, Andrews JG. Actions of hip muscles. *Phys Ther* 66: 351–359, 1986. doi:10.1093/ptj/66.3.351.

Fenn WO. Work against gravity and work due to velocity changes in running. *Am J Physiol* 93: 433–462, 1930. doi:10.1152/ajplegacy.1930.93.2.433.

Forssberg H. Ontogeny of human locomotor control. I. Infant stepping, supported locomotion and transition to independent locomotion. *Exp Brain Res* 57: 480–493, 1985. doi:10.1007/BF00237835.

Franz JR, Kram R. Advanced age and the mechanics of uphill walking: a joint-level, inverse dynamic analysis. *Gait Posture* 39: 135–140, 2014. doi:10.1016/j.gaitpost.2013.06.012.

Gerasimenko Y, Gorodnichev R, Puhov A, Moshonkina T, Savochin A, Selionov V, Roy RR, Lu DC, Edgerton VR. Initiation and modulation of locomotor circuitry output with multisite transcutaneous electrical stimulation of the spinal cord in noninjured humans. *J Neurophysiol* 113: 834–842, 2015. doi:10.1152/jn.00609.2014.

Gill ML, Grahn PJ, Calvert JS, Linde MB, Lavrov IA, Strommen JA, Beck LA, Sayenko DG, Van Straaten MG, Drubach DI, Veith DD, Thoreson AR, Lopez C, Gerasimenko YP, Edgerton VR, Lee KH, Zhao KD. Neuromodulation of lumbosacral spinal networks enables independent stepping after complete paraplegia. *Nat Med* 24: 1677–1682, 2018. [Erratum in *Nat Med* 24: 1942, 2018.] doi:10.1038/s41591-018-0175-7.

Gizzi L, Nielsen JF, Felici F, Ivanenko YP, Farina D. Impulses of activation but not motor modules are preserved in the locomotion of subacute stroke patients. *J Neurophysiol* 106: 202–210, 2011. doi:10.1152/jn.00727.2010.

Gosseye TP, Willems PA, Heglund NC. Biomechanical analysis of running in weightlessness on a treadmill equipped with a subject loading system. *Eur J Appl Physiol* 110: 709–728, 2010. doi:10.1007/s00421-010-1549-9.

Grasso R, Ivanenko YP, Zago M, Molinari M, Scivoletto G, Castellano V, Macellari V, Lacquaniti F. Distributed plasticity of locomotor pattern generators in spinal cord injured patients. *Brain* 127: 1019–1034, 2004. doi:10.1093/brain/awh115.

Grillner S. Control of locomotion in bipeds, tetrapods, and fish. In: *Handbook of Physiology. The Nervous System*. Motor Control, Part 2, edited by Brooks VB. Bethesda, MD: American Physiological Society, 1981, 1179–1235. doi:10.1002/cphy.cp010226

Hägglund M, Dougherty KJ, Borgius L, Itohara S, Iwasato T, Kiehn O. Optogenetic dissection reveals multiple rhythmogenic modules underlying locomotion. *Proc Natl Acad Sci USA* 110: 11589–11594, 2013. doi:10.1073/pnas.1304365110.

Honert EC, Zelik KE. Foot and shoe responsible for majority of soft tissue work in early stance of walking. *Hum Mov Sci* 64: 191–202, 2019. doi:10.1016/j.humov.2019.01.008.

Hunter LC, Hendrix EC, Dean JC. The cost of walking downhill: is the preferred gait energetically optimal? *J Biomech* 43: 1910–1915, 2010. doi:10.1016/j.jbiomech.2010.03.030.

Ivanenko YP, Cappellini G, Dominici N, Poppele RE, Lacquaniti F. Coordination of locomotion with voluntary movements in humans. *J Neurosci* 25: 7238–7253, 2005. doi:10.1523/JNEUROSCI.1327-05.2005.

Ivanenko YP, Cappellini G, Poppele RE, Lacquaniti F. Spatiotemporal organization of alpha-motoneuron activity in the human spinal cord during different gaits and gait transitions. *Eur J Neurosci* 27: 3351–3368, 2008. doi:10.1111/j.1460-9568.2008.06289.x.

Ivanenko YP, Cappellini G, Solopova IA, Grishin AA, Maclellan MJ, Poppele RE, Lacquaniti F. Plasticity and modular control of locomotor patterns in neurological disorders with motor deficits. *Front Comput Neurosci* 7: 123, 2013a. doi:10.3389/fncom.2013.00123.

Ivanenko YP, Dominici N, Cappellini G, Di Paolo A, Giannini C, Poppele RE, Lacquaniti F. Changes in the spinal segmental motor output for stepping during development from infant to adult. *J Neurosci* 33: 3025–3036, 2013b. doi:10.1523/JNEUROSCI.2722-12.2013.

Ivanenko YP, Poppele RE, Lacquaniti F. Spinal cord maps of spatiotemporal alpha-motoneuron activation in humans walking at different speeds. *J Neurophysiol* 95: 602–618, 2006a. doi:10.1152/jn.00767.2005.

Ivanenko YP, Poppele RE, Lacquaniti F. Motor control programs and walking. *Neuroscientist* 12: 339–348, 2006b. doi:10.1177/1073858406287987.

Janshen L, Santuz A, Ekizos A, Arampatzis A. Modular control during incline and level walking in humans. *J Exp Biol* 220: 807–813, 2017. doi:10.1242/jeb.148957.

Jessell TM, Sürmeli G, Kelly JS. Motor neurons and the sense of place. *Neuron* 72: 419–424, 2011. doi:10.1016/j.neuron.2011.10.021.

Kawamura K, Tokuhiro A, Takechi H. Gait analysis of slope walking: a study on step length, stride width, time factors and deviation in the center of pressure. *Acta Med Okayama* 45: 179–184, 1991. doi:10.18926/AMO/32212.

Kendall F, McCreary E, Provance P, Rodgers M, Romani W. *Muscles. Testing and Function with Posture and Pain* (5th North American ed.). Baltimore, MD: Lippincott Williams and Wilkins, 2005.

Kendall FP, McCreary EK, Provance PG, Rodgers MM, Romani WA. *Muscles: Testing and Function with Posture and Pain* (4th ed.). Baltimore, MD: Lippincott Williams and Wilkins, 1993.

Kiehn O. Decoding the organization of spinal circuits that control locomotion. *Nat Rev Neurosci* 17: 224–238, 2016. doi:10.1038/nrn.2016.9.

Kuo AD. Energetics of actively powered locomotion using the simplest walking model. *J Biomech Eng* 124: 113–120, 2001. doi:10.1115/1.1427703.

La Scaleia V, Ivanenko YP, Zelik KE, Lacquaniti F. Spinal motor outputs during step-to-step transitions of diverse human gaits. *Front Hum Neurosci* 8: 305, 2014. doi:10.3389/fnhum.2014.00305.

Lacquaniti F, Ivanenko YP, Zago M. Patterned control of human locomotion. *J Physiol* 590: 2189–2199, 2012. doi:10.1113/jphysiol.2011.215137.

Lange GW, Hintermeister RA, Schlegel T, Dillman CJ, Steadman JR. Electromyographic and kinematic analysis of graded treadmill walking and the implications for knee rehabilitation. *J Orthop Sports Phys Ther* 23: 294–301, 1996. doi:10.2519/jospt.1996.23.5.294.

Lay AN, Hass CJ, Gregor RJ. The effects of sloped surfaces on locomotion: a kinematic and kinetic analysis. *J Biomech* 39: 1621–1628, 2006. doi:10.1016/j.jbiomech.2005.05.005.

Lay AN, Hass CJ, Richard Nichols T, Gregor RJ. The effects of sloped surfaces on locomotion: an electromyographic analysis. *J Biomech* 40: 1276–1285, 2007. doi:10.1016/j.jbiomech.2006.05.023.

Lee DD, Seung HS. Algorithms for non-negative matrix factorization. In: *Advances in Neural Information Processing Systems 13: Proceedings of the 2000 Conference*, edited by Leen TK, Dietterich TG, Tresp V. Cambridge, MA: MIT Press, 2001.

MacLellan MJ, Ivanenko YP, Cappellini G, Sylos Labini F, Lacquaniti F. Features of hand-foot crawling behavior in human adults. *J Neurophysiol* 107: 114–125, 2012. doi:10.1152/jn.00693.2011.

MacLellan MJ, Ivanenko YP, Massaad F, Bruijn SM, Duysens J, Lacquaniti F. Muscle activation patterns are bilaterally linked during split-belt treadmill walking in humans. *J Neurophysiol* 111: 1541–1552, 2014. doi:10.1152/jn.00437.2013.

Marsh RL, Ellerby DJ, Carr JA, Henry HT, Buchanan CI. Partitioning the energetics of walking and running: swinging the limbs is expensive. *Science* 303: 80–83, 2004. doi:10.1126/science.1090704.

Martinez-Valdes E, Negro F, Falla D, De Nunzio AM, Farina D. Surface electromyographic amplitude does not identify differences in neural drive to synergistic muscles. *J Appl Physiol (1985)* 124: 1071–1079, 2018. doi:10.1152/japplphysiol.01115.2017.

Martino G, Ivanenko Y, Serrao M, Ranavolo A, Draicchio F, Rinaldi M, Casali C, Lacquaniti F. Differential changes in the spinal segmental locomotor output in hereditary spastic paraplegia. *Clin Neurophysiol* 129: 516–525, 2018. doi:10.1016/j.clinph.2017.11.028.

Martino G, Ivanenko YP, d'Avella A, Serrao M, Ranavolo A, Draicchio F, Cappellini G, Casali C, Lacquaniti F. Neuromuscular adjustments of gait associated with unstable conditions. *J Neurophysiol* 114: 2867–2882, 2015. doi:10.1152/jn.00029.2015.

McLean DL, Masino MA, Koh IY, Lindquist WB, Fetcho JR. Continuous shifts in the active set of spinal interneurons during changes in locomotor speed. *Nat Neurosci* 11: 1419–1429, 2008. doi:10.1038/nn.2225.

Merkulyeva N, Veshchitskii A, Gorsky O, Pavlova N, Zelenin PV, Gerasimenko Y, Deliagina TG, Musienko P. Distribution of spinal neuronal networks controlling forward and backward locomotion. *J Neurosci* 38: 4695–4707, 2018. doi:10.1523/JNEUROSCI.2951-17.2018.

Meurisse GM, Dierick F, Schepens B, Bastien GJ. Determination of the vertical ground reaction forces acting upon individual limbs during healthy and clinical gait. *Gait Posture* 43: 245–250, 2016. doi:10.1016/j.gaitpost.2015.10.005.

Minassian K, Hofstoetter US, Dzeladini F, Guertin PA, Ijspeert A. The human central pattern generator for locomotion: does it exist and contribute to walking? *Neuroscientist* 23: 649–663, 2017. doi:10.1177/1073858417699790.

Minetti AE, Ardigò LP, Saibene F. Mechanical determinants of gradient walking energetics in man. *J Physiol* 472: 725–735, 1993. doi:10.1113/jphysiol.1993.sp019969.

Monaco V, Ghionzoli A, Micera S. Age-related modifications of muscle synergies and spinal cord activity during locomotion. *J Neurophysiol* 104: 2092–2102, 2010. doi:10.1152/jn.00525.2009.

O'Donovan MJ, Bonnot A, Mentis GZ, Arai Y, Chub N, Shneider NA, Wenner P. Imaging the spatiotemporal organization of neural activity in the developing spinal cord. *Dev Neurobiol* 68: 788–803, 2008. doi:10.1002/dneu.20620.

Olree KS, Vaughan CL. Fundamental patterns of bilateral muscle activity in human locomotion. *Biol Cybern* 73: 409–414, 1995. doi:10.1007/BF00201475.

Pickle NT, Grabowski AM, Auyang AG, Silverman AK. The functional roles of muscles during sloped walking. *J Biomech* 49: 3244–3251, 2016. doi:10.1016/j.jbiomech.2016.08.004.

Pierotti SE, Brand RA, Gabel RH, Pedersen DR, Clarke WR. Are leg electromyogram profiles symmetrical? *J Orthop Res* 9: 720–729, 1991. doi:10.1002/jor.1100090512.

Rozumalski A, Steele KM, Schwartz MH. Muscle synergies are similar when typically developing children walk on a treadmill at different speeds and slopes. *J Biomech* 64: 112–119, 2017. doi:10.1016/j.jbiomech.2017.09.002.

Saito A, Tomita A, Ando R, Watanabe K, Akima H. Similarity of muscle synergies extracted from the lower limb including the deep muscles between level and uphill treadmill walking. *Gait Posture* 59: 134–139, 2018. doi:10.1016/j.gaitpost.2017.10.007.

Saltiel P, d'Avella A, Wyler-Duda K, Bizzi E. Synergy temporal sequences and topography in the spinal cord: evidence for a traveling wave in frog locomotion. *Brain Struct Funct* 221: 3869–3890, 2016. doi:10.1007/s00429-015-1133-5.

Santuz A, Ekizos A, Eckardt N, Kibele A, Arampatzis A. Challenging human locomotion: stability and modular organisation in unsteady conditions. *Sci Rep* 8: 2740, 2018. doi:10.1038/s41598-018-21018-4.

Sartori M, Gizzi L, Lloyd DG, Farina D. A musculoskeletal model of human locomotion driven by a low dimensional set of impulsive excitation primitives. *Front Comput Neurosci* 7: 79, 2013. doi:10.3389/fncom.2013.00079.

Selionov VA, Ivanenko YP, Solopova IA, Gurfinkel VS. Tonic central and sensory stimuli facilitate involuntary air-stepping in humans. *J Neurophysiol* 101: 2847–2858, 2009. doi:10.1152/jn.90895.2008.

Sharrard WJ. The segmental innervation of the lower limb muscles in man. *Ann R Coll Surg Engl* 35: 106–122, 1964.

Smith JL, Carlson-Kuhta P, Trank TV. Forms of forward quadrupedal locomotion. III. A comparison of posture, hindlimb kinematics, and motor patterns for downslope and level walking. *J Neurophysiol* 79: 1702–1716, 1998. doi:10.1152/jn.1998.79.4.1702.

Solopova IA, Sukhotina IA, Zhvansky DS, Ikoeva GA, Vissarionov SV, Baindurashvili AG, Edgerton VR, Gerasimenko YP, Moshonkina TR. Effects of spinal cord stimulation on motor functions in children with cerebral palsy. *Neurosci Lett* 639: 192–198, 2017. doi:10.1016/j.neulet.2017.01.003.

Stewart JD. Electrophysiological mapping of the segmental anatomy of the muscles of the lower extremity. *Muscle Nerve* 15: 965–966, 1992. doi:10.1002/mus.880150816.

Sun J, Walters M, Svensson N, Lloyd D. The influence of surface slope on human gait characteristics: a study of urban pedestrians walking on an inclined surface. *Ergonomics* 39: 677–692, 1996. doi:10.1080/00140139608964489.

Taccola G, Sayenko D, Gad P, Gerasimenko Y, Edgerton VR. And yet it moves: recovery of volitional control after spinal cord injury. *Prog Neurobiol* 160: 64–81, 2018. doi:10.1016/j.pneurobio.2017.10.004.

Tomlinson BE, Irving D. The numbers of limb motor neurons in the human lumbosacral cord throughout life. *J Neurol Sci* 34: 213–219, 1977. doi:10.1016/0022-510X(77)90069-7.

Torres-Oviedo G, Macpherson JM, Ting LH. Muscle synergy organization is robust across a variety of postural perturbations. *J Neurophysiol* 96: 1530–1546, 2006. doi:10.1152/jn.00810.2005.

van der Kruk E, van der Helm FC, Veeger HE, Schwab AL. Power in sports: a literature review on the application, assumptions, and terminology of mechanical power in sport research. *J Biomech* 79: 1–14, 2018. doi:10.1016/j.jbiomech.2018.08.031.

Wagner FB, Mignardot JB, Le Goff-Mignardot CG, Demesmaeker R, Komi S, Capogrosso M, Rowald A, Seáñez I, Caban M, Pirondini E, Vat M, McCracken LA, Heimgartner R, Fodor I, Watrin A, Seguin P, Paoles E, Van Den Keybus K, Eberle G, Schurch B, Pralong E, Becce F, Prior J, Buse N, Buschman R, Neufeld E, Kuster N, Carda S, von Zitzewitz J, Delattre V, Denison T, Lambert H, Minassian K, Bloch J, Courtine G. Targeted neurotechnology restores walking in humans with spinal cord injury. *Nature* 563: 65–71, 2018. doi:10.1038/s41586-018-0649-2.

Ward SR, Eng CM, Smallwood LH, Lieber RL. Are current measurements of lower extremity muscle architecture accurate? *Clin Orthop Relat Res* 467: 1074–1082, 2009. doi:10.1007/s11999-008-0594-8.

Warp E, Agarwal G, Wyart C, Friedmann D, Oldfield CS, Conner A, Del Bene F, Arrenberg AB, Baier H, Isacoff EY. Emergence of patterned activity in the developing zebrafish spinal cord. *Curr Biol* 22: 93–102, 2012. doi:10.1016/j.cub.2011.12.002.

Wenger N, Moraud EM, Gandar J, Musienko P, Capogrosso M, Baud L, Le Goff CG, Barraud Q, Pavlova N, Dominici N, Minev IR, Asboth L, Hirsch A, Duis S, Kreider J, Mortera A, Haverbeck O, Kraus S, Schmitz F, DiGiovanna J, van den Brand R, Bloch J, Detemple P, Lacour SP, Bézard E, Micera S, Courtine G. Spatiotemporal neuromodulation therapies engaging muscle synergies improve motor control after spinal cord injury. *Nat Med* 22: 138–145, 2016. doi:10.1038/nm.4025.

Willems PA, Cavagna GA, Heglund NC. External, internal and total work in human locomotion. *J Exp Biol* 198: 379–393, 1995.

Winter DA. *The Biomechanics and Motor Control of Human Gait: Normal, Elderly and Pathological*. Waterloo, ON, Canada: Waterloo Biomechanics, 1991.

Yakovenko S, Mushahwar V, VanderHorst V, Holstege G, Prochazka A. Spatiotemporal activation of lumbosacral motoneurons in the locomotor step cycle. *J Neurophysiol* 87: 1542–1553, 2002. doi:10.1152/jn.00479.2001.

Yang Z, Qu F, Liu H, Jiang L, Cui C, Rietdyk S. The relative contributions of sagittal, frontal, and transverse joint works to self-paced incline and decline slope walking. *J Biomech* 92: 35–44, 2019. doi:10.1016/j.jbiomech.2019.05.027.

Yokoyama H, Ogawa T, Shinya M, Kawashima N, Nakazawa K. Speed dependency in α-motoneuron activity and locomotor modules in human locomotion: indirect evidence for phylogenetically conserved spinal circuits. *Proc Biol Sci* 284: 20170290, 2017. doi:10.1098/rspb.2017.0290.

Zajac FE, Neptune RR, Kautz SA. Biomechanics and muscle coordination of human walking: part II: lessons from dynamical simulations and clinical implications. *Gait Posture* 17: 1–17, 2003. doi:10.1016/S0966-6362(02)00069-3.

Zelik KE, Adamczyk PG. A unified perspective on ankle push-off in human walking. *J Exp Biol* 219: 3676–3683, 2016. doi:10.1242/jeb.140376.

Zelik KE, Kuo AD. Human walking isn't all hard work: evidence of soft tissue contributions to energy dissipation and return. *J Exp Biol* 213: 4257–4264, 2010. doi:10.1242/jeb.044297.

Zelik KE, Kuo AD. Mechanical work as an indirect measure of subjective costs influencing human movement. *PLoS One* 7: e31143, 2012. doi:10.1371/journal.pone.0031143.

Zelik KE, La Scaleia V, Ivanenko YP, Lacquaniti F. Can modular strategies simplify neural control of multidirectional human locomotion? *J Neurophysiol* 111: 1686–1702, 2014. doi:10.1152/jn.00776.2013.

Zelik KE, La Scaleia V, Ivanenko YP, Lacquaniti F. Coordination of intrinsic and extrinsic foot muscles during walking. *Eur J Appl Physiol* 115: 691–701, 2015. doi:10.1007/s00421-014-3056-x.